Pnictogen height as a possible switch between high-T_c nodeless and low-T_c nodal pairings in the iron-based superconductors

Kazuhiko Kuroki,[1,2] Hidetomo Usui,[1] Seiichiro Onari,[2,3] Ryotaro Arita,[2,4,5] and Hideo Aoki[2,6]
[1]*Department of Applied Physics and Chemistry, The University of Electro-Communications, Chofu, Tokyo 182-8585, Japan*
[2]*JST, TRIP, Sanbancho, Chiyoda, Tokyo 102-0075, Japan*
[3]*Department of Applied Physics, Nagoya University, Nagoya 464-8603, Japan*
[4]*Department of Applied Physics, University of Tokyo, Hongo, Tokyo 113-8656, Japan*
[5]*JST, CREST, Hongo, Tokyo 113-8656, Japan*
[6]*Department of Physics, University of Tokyo, Hongo, Tokyo 113-0033, Japan*
(Received 16 April 2009; revised manuscript received 17 May 2009; published 10 June 2009)

We study the effect of the lattice structure on the spin-fluctuation-mediated superconductivity in the iron pnictides adopting the five-band models of several virtual lattice structures of LaFeAsO, as well as actual materials such as NdFeAsO and LaFePO obtained from the maximally localized Wannier orbitals. Random phase approximation is applied to the models to solve the Eliashberg equation. This reveals that the gap function and the strength of the superconducting instability are determined by the cooperation or competition among multiple spin-fluctuation modes arising from several nestings among disconnected pieces of the Fermi surface, which is affected by the lattice structure. Specifically, the appearance of the Fermi surface γ around (π,π) in the unfolded Brillouin zone is sensitive to the pnictogen height h_{Pn} measured from the Fe plane, where h_{Pn} is shown to act as a switch between high-T_c nodeless and low-T_c nodal pairings. We also find that reduction in the lattice constants generally suppresses superconductivity. We can then combine these to obtain a generic superconducting phase diagram against the pnictogen height and lattice constant. This suggests that NdFeAsO is expected to exhibit a fully gapped, sign-reversing s-wave superconductivity with a higher T_c than in LaFeAsO, while a nodal pairing with a low T_c is expected for LaFePO, which is consistent with experiments.

DOI: 10.1103/PhysRevB.79.224511 PACS number(s): 74.20.Mn, 74.20.Rp, 74.62.Bf

I. INTRODUCTION

The discovery of superconductivity in the iron-based compounds by Hosono's group[1] and subsequent increase in the transition temperature (T_c) exceeding 50 K (Ref. 2) in the same family of compounds are seminal not only because of high values of T_c, but also because this poses a fundamental question on electronic mechanisms of high-T_c superconductivity in a wider class of compounds other than cuprates.

Theoretically, a phonon mechanism was shown to be unlikely for this system,[3] and a spin-fluctuation-mediated pairing has been proposed from the very early stage of the study.[4–6] In these studies the nesting between disconnected pieces (pockets) of the Fermi surface is shown to induce spin fluctuations associated with the nesting vector. This can give rise to a superconducting gap, which is basically s wave but changes sign between different pockets, hence termed as $s\pm$ wave or sign-reversing s-wave first proposed by Mazin *et al.*[4] (see Fig. 4). Although recent experimental as well as theoretical studies suggest that the magnetism in the *undoped* material is not driven solely by Fermi-surface nesting,[6] the spin fluctuation originating from the nesting has been considered to be a possible origin of the pairing interaction by a number of authors.[5,7–18]

In particular, the present authors with Tanaka and Kontani have constructed a minimal model, which has turned out to be five-band one, for LaFeAsO based on first-principles calculation, and investigated spin-fluctuation-mediated superconductivity with random-phase approximation (RPA).[5,19–21] In that study it was pointed out that along with the sign-reversing s wave, a d-wave pairing can also be a candidate depending on the band filling. Our five-band model has subsequently been adopted in various studies, among which are a perturbation study by Nomura,[12] a fluctuation exchange study by Ikeda,[13] and a functional renormalization-group study by Wang *et al.*[14] An analysis on the normal-state spin dynamics has also been performed using our five-band model,[22] where good agreement with inelastic-neutron-scattering experiments[23,24] has been obtained. On the other hand, Graser *et al.*[25,26] recently applied RPA to a five-band model that is based on a band structure obtained by Cao *et al.*[27] The study finds that a sign-reversing s wave that has nodes intersecting the Fermi surface closely competes with d-wave pairing (see Fig. 4). It has further been proposed in Ref. 28 that this nodal s-wave pairing is intrinsic to the iron pnictide superconductors, while a full gap can occur as a consequence of the presence of impurities. It is also worth noting that a competition or mixture of sign-reversing s and d pairings have also been discussed on the basis of a 16-band d-p model[17] and a two-orbital exchange coupling model (J_1-J_2 model).[29] It is the purpose of the present paper to explore systematically the material and structure dependences on the strength and gap symmetry of superconductivity in terms of the five-band model. Experimentally, the fully gapped, sign-reversing s-wave scenario is consistent with a number of measurements on arsenides, such as angle-resolved photoemission spectroscopy (ARPES),[30,31] penetration depth measurements,[32] and muon spin relaxation (μSR),[33–36] which suggest that the gap is open on the whole Fermi surface, although the magnitude of the gap may vary along the surface. The fully gapped, sign-reversing s is also consistent with some neutron-scattering results[37,38] that ob-

serve a resonance peak predicted theoretically.[39–41] On the other hand, the weak effect of nonmagnetic impurities such as Co on T_c (Ref. 42) or even the appearance of superconductivity upon Co doping[43–45] has cast doubt on the sign-reversing gap, but some theoretical studies[46–48] have shown that these experiments in fact do not necessarily contradict with the $s\pm$. In particular, Senga and Kontani showed that the effect of the interpocket scattering due to nonmagnetic impurities becomes irrelevant in the unitarity limit.[47,48]

One interesting and important feature in the iron pnictides is the unusually strong dependence of T_c on materials, which ranges from $\simeq$5 K in LaFePO (Ref. 49) to 55 K in SmFeAsO (Ref. 2) even within the same group of elements. More systematically, Lee *et al.*[50] pointed out that we can parametrize the value of T_c in terms of the Fe-Pn-Fe (Pn: pnictogen) bond angle α, where T_c seems to have a peak around the bond angle ($\simeq$109) at which the pnictogens form a regular tetrahedron, while T_c is low for materials with large α such as LaFePO. The importance of the bond angle has also been pointed out by Zhao *et al.*[51] On the other hand, it has also been shown by Miyazawa *et al.* that the chemical trend for LnFeAsO has the maximum T_c increasing with the decreasing lattice constant a for Ln=La$\rightarrow$Nd, but nearly constant for Ln=Nd$\rightarrow$Dy.[52] Pressure effects have also been experimentally elaborated. For LaFeAsO, T_c first increases with pressure, but then decreases when the pressure becomes too large,[53–56] which is contrasted with materials having T_c $>$50 K at ambient pressure such as NdFeAsO for which T_c monotonically and rapidly decreases with pressure.[57] All these experimental results indicate that T_c is unusually sensitive to the lattice structure in the iron-based compounds.

If we move on to the symmetry of the superconducting gap, we have various pieces of experimental evidence for strong material dependence as well: while a number of experiments on arsenides suggests that the gap is fully open on the Fermi surface as mentioned, a recent penetration depth measurement on LaFePO shows that there are nodes in the superconducting gap.[58,59] Arsenides and LaFePO also exhibit sharp contrast in nuclear-magnetic-resonance (NMR) experiments. In LaFeAsO, some experiments show that the NMR relaxation rate $1/T_1$ has no coherence peaks, and decays as T^3 below T_c,[60–65] while a recent experiment by Kobayashi *et al.*[66] indicates a more rapid decay. In LaFePO, $1/T_1$ below T_c is shown to decay even more slowly than above T_c.[67] These results strongly suggest that even the symmetry of the superconducting gap can be unusually sensitive to the lattice structure.

So the crucial theoretical question is how we can understand these sensitivities. In analyzing the structure dependence, there is one factor to which we have to pay attention. Previous theoretical studies have shown that the position of the pnictogen with respect to the Fe plane affects the band structure, in particular the character of the bands that lie close to the Fermi level near the Γ point (in the folded Brillouin zone) as well as the band width (see Fig. 7).[68–70] Local spin-density approximation studies have shown that the tendency toward magnetism becomes stronger when the pnictogen lies farther from the Fe plane, which is expected to enhance superconductivity if the pairing is mediated by spin fluctuations.[71]

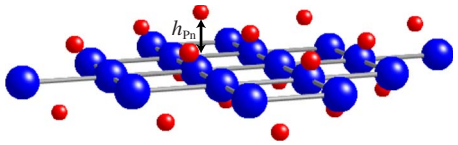

FIG. 1. (Color online) Lattice structure of one Fe-Pn layer, with the pnictogen height indicated.

Given this background, in the present study we investigate the lattice structure dependence of the spin-fluctuation-mediated superconductivity, where we construct five-band models for several virtual lattice structures of LaFeAsO as well as actual materials such as NdFeAsO and LaFePO, and apply RPA to solve the Eliashberg equation. We shall show that the position of the pnictogen is indeed the key factor that determines both T_c *and* the form of the superconducting gap, namely, the "pnictogen height" above the Fe plane (Fig. 1) can act as a *switch between a high-*T_c fully gapped sign-reversing s-wave and a low-T_c nodal (s- or d-wave) pairings. We also show that the reduction in the lattice constant is generally unfavorable for superconductivity. Combining these results for the lattice structure dependence, we then obtain a generic "phase diagram" against the pnictogen height and the lattice constants. Based on the phase diagram, we argue that the systematic dependence of T_c against the bond angle found in Ref. 50 can be accounted for as a combined effect of the pnictogen height and the lattice constants. In order to get higher T_c, we propose to seek for materials that have high position of the pnictogen and large lattice constants simultaneously.

II. BAND STRUCTURE AND THE FERMI SURFACE

LaFeAsO has a tetragonal layered structure, where Fe atoms form a square lattice in each layer, which is sandwiched by As atoms [Figs. 1 and 2(a)]. Due to the tetrahedral coordination of As, there are two Fe atoms per unit cell. The experimentally determined lattice constants are a=4.036 Å and c=8.739 Å, with two internal coordinates z_{La}=0.142 and z_{As}=0.6512.[1] We have obtained the band structure [Fig. 2(b)] with the local-density approximation with a plane-wave basis.[72] We then construct the maximally localized Wannier functions (MLWFs).[73] These MLWFs, centered at the two Fe sites in the unit cell, have five-orbital symmetries [$d_{3Z^2-R^2}$, d_{XZ}, d_{YZ}, $d_{X^2-Y^2}$, and d_{XY}, where X,Y,Z refer to those for the unit cell with two Fe sites as shown in Fig. 2(a)]. The two Wannier orbitals in each unit cell are equivalent in that each Fe atom has the same local arrangement of surrounding atoms. We can then take a unit cell that contains only one orbital (for each orbital symmetry) by unfolding the Brillouin zone, and we end up with an effective five-band model on a square lattice, where x and y axes are rotated by 45 degrees from X-Y, to which we refer for all the wave vectors hereafter. We define the band filling n as the number of electrons/number of sites (e.g., n=10 for a full filling). The doping level x in $LaFeAsO_{1-x}F_x$ is related to the band filling as $n=6+x$.

The five bands are heavily entangled as shown in Fig. 2(b), reflecting the strong hybridization of the five 3d orbit-

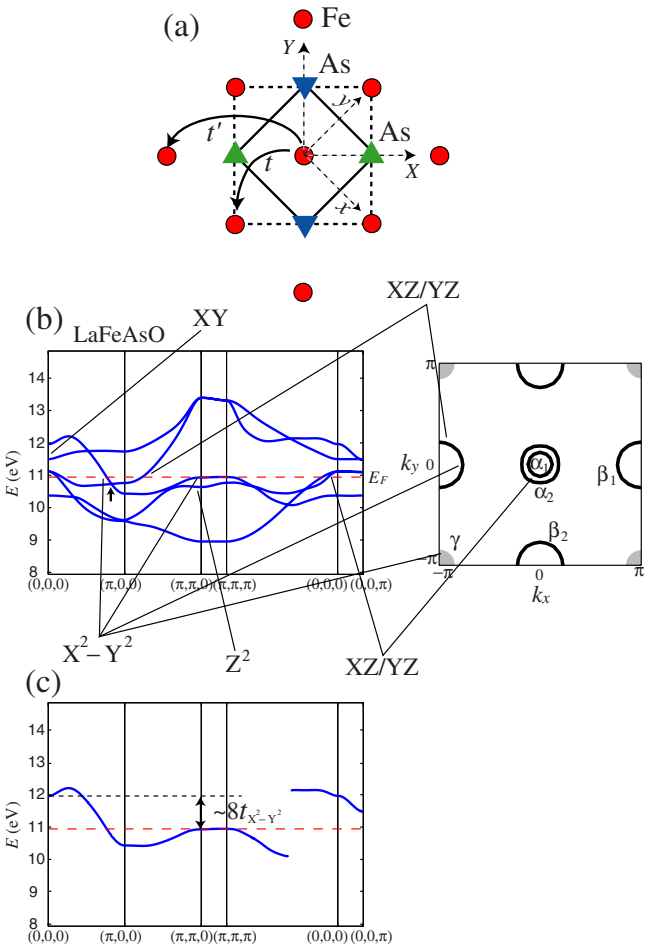

FIG. 2. (Color online) (a) The original (dashed lines) and reduced (solid) unit cells with ● (Fe), ▽ (As below the Fe plane) and △ (above Fe). (b) The band structure (left) of the five-band model for LaFeAsO, and the Fermi surface (right) at $k_z=0$ for $n=6.1$. The main orbital characters of some portions of the bands and the Fermi surface are indicated. The dashed horizontal line in the band structure indicates the Fermi level for $n=6.1$. The short arrow in the band structure indicates the position of the Dirac cone closest to the Fermi level. The gray areas in the Fermi surface around the zone corners represent the γ Fermi surface. (c) The portion of the band that has mainly the $d_{X^2-Y^2}$ orbital character.

als, which is physically due to the tetrahedral coordination of As atoms around Fe. Hence we conclude that the minimal electronic model requires all the five bands.[19] In Fig. 2(b), the Fermi surface at $k_z=0$ for $n=6.1$ (corresponding to $x=0.1$) is shown in the unfolded Brillouin zone. The Fermi surface consists of four pieces [pockets in two dimensions (2D)]: two concentric hole pockets (denoted as α_1, α_2) around $(k_x,k_y)=(0,0)$ and two electron pockets around $(\pi,0)$ (β_1) or $(0,\pi)$ (β_2), respectively. Besides these pieces of the Fermi surface, there is a portion of the band around (π,π) that touches the E_F at $n=6.1$ so that this portion acts as a "quasi Fermi surface" (which we call γ). As for the orbital character, α and some portions of β near the Brillouin-zone edge have mainly d_{XZ} and d_{YZ} character, while the portions of β away from the Brillouin-zone edge and γ have mainly $d_{X^2-Y^2}$ orbital character. An interesting feature in the band structure is the presence of Dirac cones, i.e., places where the upper and the lower bands make a conical contact.[20,74] The ones closest to the Fermi level correspond to the crossing points of the $d_{X^2-Y^2}$ and the d_{XZ}/d_{YZ} bands below the β Fermi surface.

III. MANY-BODY HAMILTONIAN AND RANDOM-PHASE APPROXIMATION

For the many-body part of the Hamiltonian, we consider the standard interaction terms that comprise the intraorbital Coulomb U, the interorbital Coulomb U', the Hund's coupling J, and the pair-hopping J'. The many-body Hamiltonian then reads

$$H = \sum_i \sum_\mu \sum_\sigma \varepsilon_\mu n_{i\mu\sigma} + \sum_{ij} \sum_{\mu\nu} \sum_\sigma t_{ij}^{\mu\nu} c_{i\mu\sigma}^\dagger c_{j\nu\sigma} + \sum_i \Bigg(U \sum_\mu n_{i\mu\uparrow} n_{i\mu\downarrow} + U' \sum_{\mu>\nu} \sum_{\sigma,\sigma'} n_{i\mu\sigma} n_{i\nu\sigma'} - J \sum_{\mu\neq\nu} \boldsymbol{S}_{i\mu} \cdot \boldsymbol{S}_{i\nu} + J' \sum_{\mu\neq\nu} c_{i\mu\uparrow}^\dagger c_{i\mu\downarrow}^\dagger c_{i\nu\downarrow} c_{i\nu\uparrow} \Bigg), \quad (1)$$

where i,j denote the sites and μ,ν the (five d) orbitals and $t_{ij}^{\mu\nu}$ is the obtained in the previous section. The orbitals $d_{3Z^2-R^2}$, d_{XZ}, d_{YZ}, $d_{X^2-Y^2}$, and d_{XY} are labeled as $\nu=1$, 2, 3, 4, and 5, respectively. As for the electron-electron interactions, there have been theoretical studies that estimate the parameter values. Some studies give $U=2.2-3.3$ and $J=0.3-0.6$ (Refs. 75 and 76) in units of eV, while others have $U\sim J$.[77] Here we assume that $U>J$ and take the values $U=1.2$, $U'=0.9$, and $J=J'=0.15$. We also examine orbital-dependent interactions as introduced in Sec. V C. We have taken the values somewhat smaller than those obtained in Refs. 75 and 76 because the self-energy correction is not taken into account in the present RPA calculation, so that small interaction parameters are needed to avoid magnetic ordering at high temperatures.

Having constructed the model, we move on to the five-band RPA calculation, where the modification of the band structure due to the self-energy correction is not taken into account. Multiorbital RPA is described in e.g., Refs. 78 and 79. In the present case, Green's function $G_{lm}(k)$ [$k \equiv (\boldsymbol{k}, i\omega_n)$] is a 5×5 matrix. The irreducible susceptibility matrix

$$\chi^0_{l_1,l_2,l_3,l_4}(q) = \sum_k G_{l_1 l_3}(k+q) G_{l_4 l_2}(k) \quad (2)$$

($l_i=1,\ldots,5$) has 5^4 components, and the spin and the charge (orbital) susceptibility matrices are obtained from matrix equations,

$$\hat{\chi}_s(q) = \frac{\hat{\chi}^0(q)}{1-\hat{S}\hat{\chi}^0(q)}, \quad (3)$$

$$\hat{\chi}_c(q) = \frac{\hat{\chi}^0(q)}{1+\hat{C}\hat{\chi}^0(q)}, \quad (4)$$

where

$$S_{l_1l_2,l_3l_4} = \begin{cases} U, & l_1 = l_2 = l_3 = l_4 \\ U', & l_1 = l_3 \neq l_2 = l_4 \\ J, & l_1 = l_2 \neq l_3 = l_4 \\ J', & l_1 = l_4 \neq l_2 = l_3, \end{cases} \quad (5)$$

$$C_{l_1l_2,l_3l_4} = \begin{cases} U & l_1 = l_2 = l_3 = l_4 \\ -U' + J & l_1 = l_3 \neq l_2 = l_4 \\ 2U' - J, & l_1 = l_2 \neq l_3 = l_4 \\ J' & l_1 = l_4 \neq l_2 = l_3. \end{cases} \quad (6)$$

We denote the largest eigenvalue of the spin (charge) susceptibility matrix for $i\omega_n=0$ as $\chi_s(\boldsymbol{k})[\chi_c(\boldsymbol{k})]$.

The Green's function and the effective singlet pairing interaction,

$$\hat{V}^s(q) = \frac{3}{2}\hat{S}\hat{\chi}_s(q)\hat{S} - \frac{1}{2}\hat{C}\hat{\chi}_c(q)\hat{C} + \frac{1}{2}(\hat{S} + \hat{C}), \quad (7)$$

are plugged into the linearized Eliashberg equation,

$$\lambda\phi_{l_1l_4}(k) = -\frac{T}{N}\sum_q \sum_{l_2l_3l_5l_6} V_{l_1l_2l_3l_4}(q) \times G_{l_2l_5}(k-q)\phi_{l_5l_6}(k-q)G_{l_3l_6}(q-k). \quad (8)$$

The 5×5 matrix gap function ϕ_{lm} in the orbital representation along with the associated eigenvalue λ is obtained by solving this equation. The gap function can be transformed into the band representation with a unitary transformation. The calculation is performed at $T=0.02$ eV taking a three dimensional k-point mesh of $32\times32\times4$ and 512 Matsubara frequencies. All the results for the spin susceptibility and the superconducting gap will be presented for the lowest Matsubara frequency and at $k_z=0$ or $q_z=0$. The eigenvalue of the Eliashberg equation λ at the fixed temperature of 0.02 eV will be adopted as a measure of the strength of the superconducting instability since directly obtaining T_c, especially for low-T_c systems, requires more k-point meshes and Matsubara frequencies.

IV. ORBITAL-DEPENDENT NESTING AND THE PAIRING SYMMETRY COMPETITION

Let us first look in Fig. 3 at the result for the (orbital-diagonal components of) spin susceptibility, χ_{s3333} and χ_{s4444}, which are the two largest components. χ_{s3333} has peaks solely around $(\pi,0)$ and $(0,\pi)$, which reflects the nesting between d_{XZ}, d_{YZ} portions of α and β pockets as shown in the lower panel of Fig. 3, where the thickness of the Fermi surface represents the strength of the $d_{X^2-Y^2}$ or d_{XZ}/d_{YZ} characters. On the other hand, χ_{s4444} has peaks around $(\pi,0),(0,\pi)$ and $(\pi,\pi/2),(\pi/2,\pi)$. The former is due to the nesting between the γ pocket and the $d_{X^2-Y^2}$ portion of the β pocket, while the latter originates from the nesting between the $d_{X^2-Y^2}$ portion of the β_1 and β_2.[5,21,25,26,80]

The superconducting gap should be determined by the cooperation or competition between the multiple nestings mentioned above. Specifically, the α-β and γ-β nestings tend to favor the fully gapped sign-reversing s wave, in which the gap changes sign between α and β but has a constant sign on each pocket as shown in Fig. 4.[4] On the other hand, β_1-β_2 nesting tends to change the sign of the gap between these pockets, which can result in either d-wave or an s-wave pairing with nodes on the β Fermi surface, as shown schematically in Fig. 4.[5,7,25] For the band structure of LaFeAsO (obtained by using the experimentally determined lattice structure), the sign-reversing s wave with no nodes intersecting the Fermi surface dominates for the present set of parameter values with $n=6.1$ as shown in Fig. 5.[7] The eigenvalue of the Eliashberg equation at $T=0.02$ eV is $\lambda=0.90$ for s wave, against $\lambda=0.54$ for d wave.

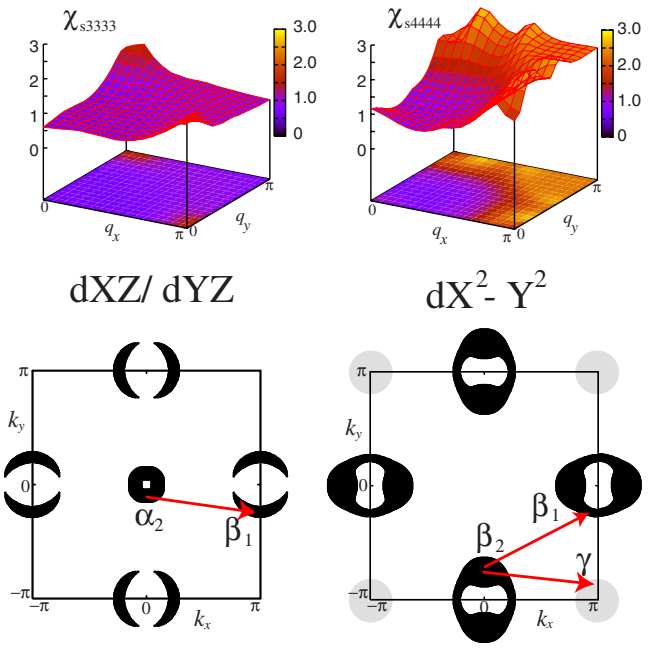

FIG. 3. (Color online) Top panels: Diagonal components, χ_{s3333} and χ_{s4444}, of the spin susceptibility matrix in the orbital representation ($3:YZ$, $4:X^2-Y^2$) for the five-band model of LaFeAsO with $n=6.1$. Bottom: Nesting is shown for the Fermi surface for orbitals XZ, YZ (left) and X^2-Y^2 (right). Here the thickness of the Fermi surface represents the strength of the respective orbital character.

As for the band-filling dependence, we plot the eigenvalue of the Eliashberg equation of s- and d-wave pairings in Fig. 6(a). We can see for the band structure of LaFeAsO with the present set of interaction values that the sign-reversing s-wave pairing with a full gap for each pocket dominates for the band filling $n\leq6.2$. For $n\geq6.3$, the γ pocket becomes less effective, and the $(\pi,0)$ peak in χ_{s4444} disappears as seen in the right panel of Fig. 6(b). The α pocket becomes less effective as well, and the $(\pi,0)$ peak in χ_{s3333} becomes small. Thus in this region, d-wave pairing begins to dominate, and the subdominant s-wave gap has nodes almost touching the β as seen in the right panel of Fig. 6(c). For small doping levels when the γ Fermi surface is effective and s-wave dominates, the magnitude of the s-wave gap has maxima at the positions along the β pocket facing the Γ point (Fig. 5, lower left), but when the doping increases to $n=6.3$, the s-wave gap has minima at these points. The gap turns out to be nearly constant on the β Fermi surface [Fig. 6(c), left] for the band filling $n\simeq6.2$. In this case, the gap on

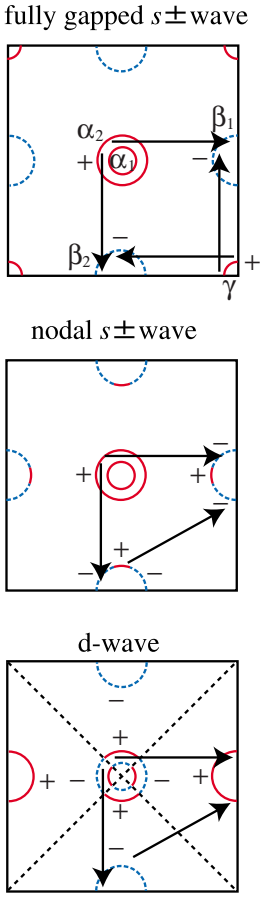

FIG. 4. (Color online) The fully gapped $s\pm$ wave (top panel), the nodal $s\pm$ wave (middle), and the d-wave gap (bottom) are schematically shown. The solid red (dashed blue) curves represent positive (negative) sign of the gap. The arrows indicate the dominating nesting vectors. γ Fermi surface is present when the pnictogen height is large.

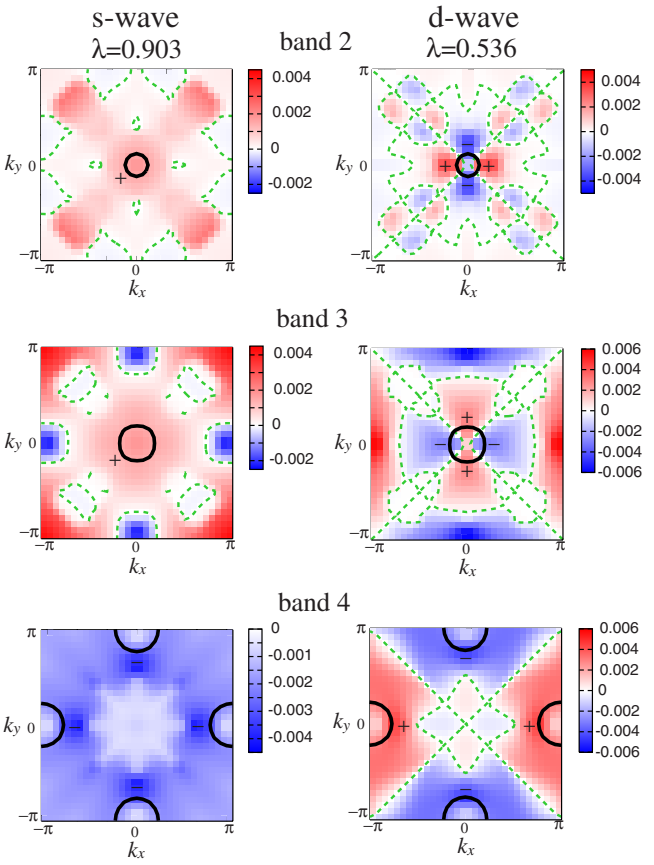

FIG. 5. (Color online) The s-wave (left panels) and d-wave (right) gap functions for the second to fourth bands from top to bottom in the band representation for the five-band model of LaFeAsO with $n=6.1$. Solid lines represent the Fermi surface, and green dashed lines the nodes in the gap.

α (not shown) and β have nearly the same magnitude.

Note however that the present analysis on the band-filling dependence does not take account of the doping dependence of the band structure itself, which should occur mainly due to the change of the As position caused by doping. We will come back to this point in Sec. VI B, taking NdFeAsO as an example.

V. EFFECT OF THE LATTICE STRUCTURE

A. Pnictogen height dependence

We now investigate the effect of the "pnictogen height h_{Pn}," namely, the distance between a pnictogen atom and the Fe layer, $(z_{\mathrm{Pn}}-0.5)\times c$, where z_{Pn} is the internal coordinate of the pnictogen atom and c the c-axis lattice constant. As shown in previous studies,[68–70] z_{Pn} controls the relative position of $d_{X^2-Y^2}(=d_{xy})$ and d_{Z^2} bands near the Γ point of the folded (original) Brillouin zone. In the unfolded Brillouin zone, these bands appear near (π,π). In Fig. 7, we show the band structure in the unfolded Brillouin zone for virtual lattice structure with $z_{\mathrm{As}}=0.658$ and 0.6304 with the lattice constants and z_{La} fixed at the original values for LaFeAsO. For the original $z_{\mathrm{As}}=0.651$, the As height is $h_{\mathrm{As}}=1.32$ Å. For $z_{\mathrm{As}}=0.658$, h_{As} increases to 1.38 Å, which is the same as in the optimally doped NdFeAsO, while $z_{\mathrm{As}}=0.6304$ ($h_{\mathrm{As}}=1.14$ Å) corresponds to the height of P in LaFePO. We see that the $d_{X^2-Y^2}$ band that forms the γ Fermi surface around (π,π) rises as h_{As} is increased, while the d_{Z^2} band sinks below the Fermi level.

The reason for these shifts in the band positions can be understood in terms of the hopping integrals. As h_{As} increases, the nearest-neighbor hopping for the $d_{X^2-Y^2}$ orbital decreases as shown in Table I. If we approximate the $d_{X^2-Y^2}$ portion of the bands by

$$\varepsilon_{X^2-Y^2}(\boldsymbol{k}) = -2t_{X^2-Y^2}[\cos(k_x)+\cos(k_y)] - 4t'_{X^2-Y^2}\cos(k_x)\cos(k_y), \quad (9)$$

where $t'_{X^2-Y^2}$ stands for the second-nearest-neighbor hopping, the energy difference between (0,0) and (π,π) is proportional to $t_{X^2-Y^2}$ [Fig. 2(c)] so that the reduction in $t_{X^2-Y^2}$ acts to push up the $d_{X^2-Y^2}$ band at (π,π). Besides the variation in the $d_{X^2-Y^2}$ hoppings, the increase in h_{As} results in an overall reduction in the hopping integrals of other orbitals because the effective hopping path Fe→As→Fe becomes less effective.

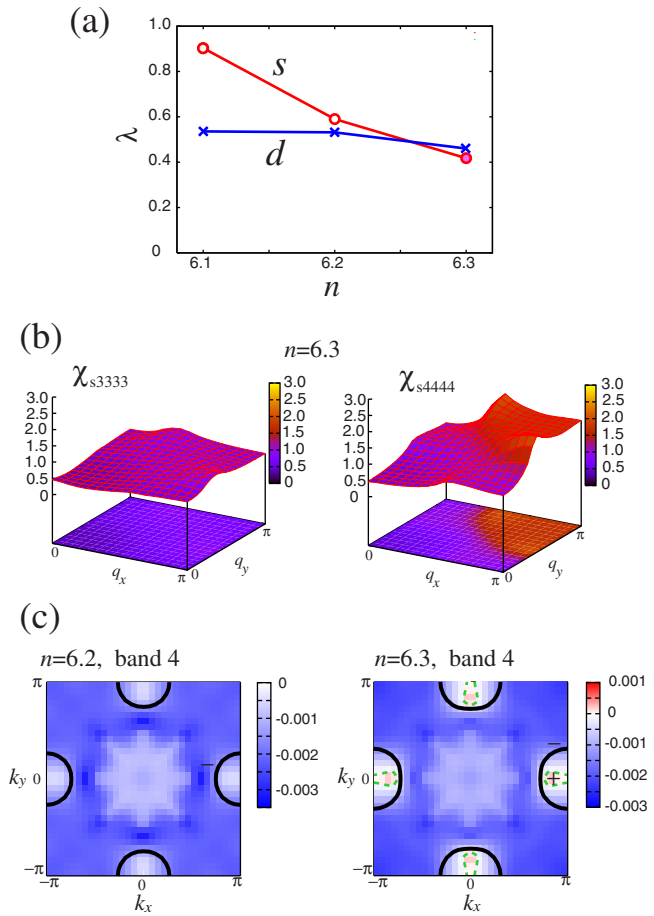

FIG. 6. (Color online) (a) Eigenvalues of the Eliashberg equation for s wave and d wave, respectively, for the five-band model of LaFeAsO plotted against the band filling n. The light red (or gray) symbol for the s wave at $n=6.3$ indicates that the gap is nearly nodal. (b) χ_{s3333} and χ_{s4444} for $n=6.3$. (c) The s-wave gap function for band 4 with $n=6.2$ (left) and $n=6.3$ (right).

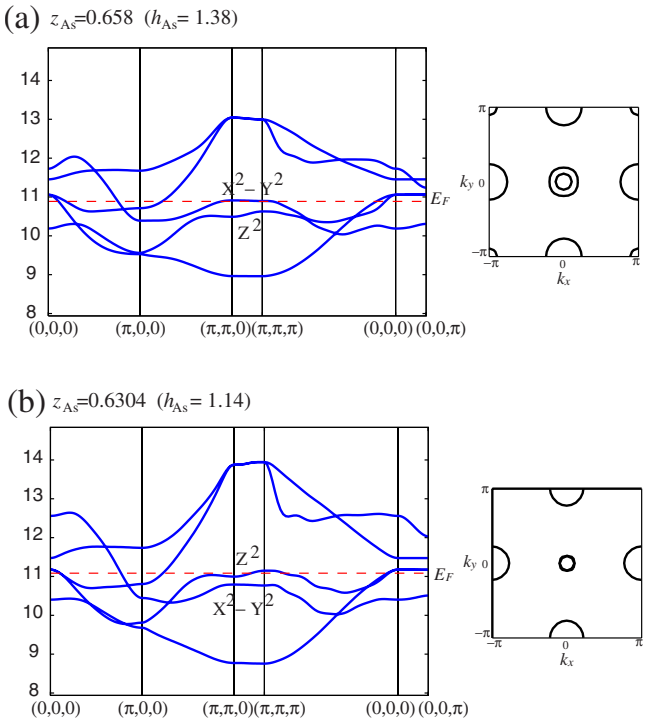

FIG. 7. (Color online) Band structure in the five-band model for (a) $z_{As}=0.658$ and (b) $z_{As}=0.6304$. The lattice constants are kept at the original values of LaFeAsO. X^2-Y^2 and Z^2 denote the main characters of the bands around (π,π,k_z). Dashed lines represent the Fermi energy, and the Fermi surface at $k_z=0$ for $n=6.1$ is shown on the right panels.

The effect of varying h_{As} on the spin susceptibility is shown in Fig. 8. The d_{YZ} orbital component always has peaks around $(\pi,0),(0,\pi)$ reflecting the α-β nesting. On the other hand, the $d_{X^2-Y^2}$ orbital component of the spin susceptibility χ_{s4444} exhibits a strong variation with h_{As}: when h_{As} is large and the γ pocket is present, χ_{s4444} [Fig. 8(a), right] is strongly peaked at $(\pi,0)$, reflecting the γ-β nesting and also the strong electron correlation due to the overall reduction in the band width. However, as h_{As} is reduced, the structure around $(\pi,\pi/2)$, which arises from the β_1-β_2 nesting, dominates [Fig. 8(b), right]. The effect of reducing h_{As} resembles the effect of electron doping, but in the case of electron doping, not only the effect of the γ pocket, but also that of the α becomes weak, so that χ_{s3333} is suppressed.

The effect on the spin susceptibility in turn affects superconductivity. When h_{As} is large, χ_{s4444} and χ_{s3333} spin fluctuations near $(\pi,0)$ *cooperate* to mediate the fully gapped sign-reversing s-wave superconductivity. When h_{As} is small, by contrast, the $(\pi,\pi/2)$ spin fluctuations begin to favor d-wave and nodal s-wave pairings. In Fig. 9, we plot against z_{As} (lower scale) or against h_{As} (upper scale) the eigenvalue of the Eliashberg equation for the s-wave and d-wave pairings, respectively. For large h_{As} where the fully gapped sign-reversing s wave (Fig. 10, upper right) dominates, λ is large because the strong spin fluctuations arising from α-β and γ-β nestings cooperate. This is contrasted with the case of small h_{As}, where d wave or nodal s wave begin to dominate (Fig. 10, left). In this region λ is small because the γ-β nesting is no longer effective, or to be more precise, its remaining effect *competes* with the effect of the β_1-β_2 nesting. It is worth noting that if we adopt $z_{As}=0.638$, which is the value determined by theoretical structure optimization,[4] we have the closely competing d-wave and nodal s-wave pairings. This is consistent with a recent RPA calculation by Graser *et al.*,[25] who adopted a band structure determined by a theoretical structure optimization.[27] The message of the present analysis, then, is that the pnictogen height can act as a "switch" between the fully gapped sign-reversing high-T_c s wave and the low-T_c gapless (either d-wave or nodal s-wave) superconductivity.

B. Lattice-constant dependence

We now turn to the effect of the lattice constants. We consider virtual lattice structures where one of the lattice constants, a or c, is varied, while the pnictogen height is fixed at the original value for LaFeAsO. When we reduce the lattice constant a, we find that the nearest-neighbor hopping $t_{X^2-Y^2}$ decreases, probably because the Fe-As-Fe angle is reduced, which may cause a suppression of the effective hop-

TABLE I. Materials and lattice structures considered in the present study, and the nearest and second-nearest-neighbor hopping integrals (in eV) in the corresponding tight-binding models. Shorthands are: La (LaFeAsO), Nd (optimally doped $NdFeAsO_{1-y}$), Nd-p ($NdFeAsO_{1-y}$ under the pressure of 3.8 GPa), Nd-ud (underdoped $NdFeAsO_{1-y}$), and P (LaFePO). The cases with $a=3.95$ Å, $c=8.40$ Å, $h_{As}=1.38$ Å, or 1.14 Å correspond to virtual structures of LaFeAsO. Note that $(z_{Pn}-0.5)\times c=h_{Pn}$.

	a (Å)	c (Å)	z_{Pn}	h_{Pn} (Å)	α	$t_{X^2-Y^2}$	$t'_{X^2-Y^2}$	t_{XZ}	t'_{XZ}
La[a]	4.04	8.74	0.6512	1.32	113.6	0.163	0.124	−0.210	0.329
$h_{As}=1.38$ Å	4.04	8.74	0.6580	1.38	111.2	0.132	0.113	−0.191	0.309
$h_{As}=1.14$ Å	4.04	8.74	0.6304	1.14	121.1	0.261	0.153	−0.240	0.364
$a=3.95$ Å	3.95	8.74	0.6512	1.32	112.4	0.148	0.123	−0.210	0.346
$c=8.40$ Å	4.04	8.40	0.6573	1.32	113.6	0.174	0.132	−0.209	0.327
Nd[b]	3.94	8.51	0.6624	1.38	109.9	0.135	0.123	−0.202	0.332
Nd-p[c]	3.92	8.37	0.6584	1.33	111.9	0.172	0.138	−0.217	0.350
Nd-ud[b]	3.97	8.57	0.6571	1.35	111.7	0.156	0.129	−0.213	0.341
P[d]	3.96	8.51	0.6339	1.14	120.2	0.253	0.156	−0.234	0.377

[a]Reference 1.
[b]Reference 50.
[c]Reference 81.
[d]Reference 49.

ping via the path Fe→As→Fe. Nonetheless, most of the other in-plane hopping integrals (including the ones not listed in the table) are enhanced as intuitively expected. On the other hand, a reduction in the lattice constant c is found to mainly enhance the in-plane $d_{X^2-Y^2}$ hopping (apart from the obvious enhancement of the hopping in the c direction). This may be because the As wave function is pushed toward the Fe plane for a reduced layer-layer distance, and the hopping between $d_{X^2-Y^2}$ orbitals, which is elongated in the direction of the As atom positions, is enhanced by this deformation.

The eigenvalue of the Eliashberg equation is plotted as functions of the lattice constants in Fig. 11. We find that the reduction in the lattice constants tends to suppress superconductivity, which can be attributed to the increased hopping integrals and associated suppression of the electron correlation. In fact, the reduction in a (c) enhances the XZ,YZ (X^2-Y^2) hopping integrals, which leads to suppressed χ_{s3333} (χ_{s4444}) as seen from the comparison between Fig. 3 and the lower panels of Fig. 11. The effect of reduced lattice constants is small for the competition between s and d waves (i.e., two curves move roughly in parallel). We note here that, although an increased h_{As} and a decreased lattice constant a both lead to a reduction in the Fe-As-Fe bond angle α, they have opposite effects on the eigenvalue of the Eliashberg equation (compare Figs. 9 and 11).

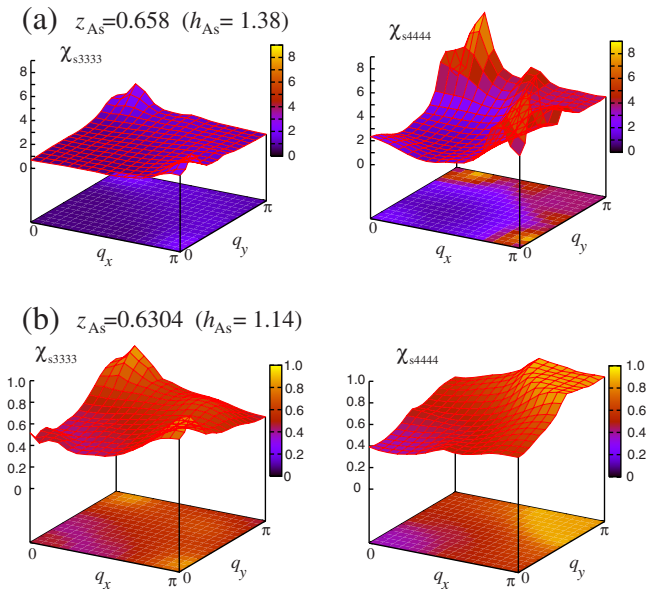

FIG. 8. (Color online) χ_{s3333} (left panels) and χ_{s4444} (right) for the model with (a) $z_{As}=0.658$ and (b) $z_{As}=0.6304$.

C. Effect of the orbital-dependent interactions

In Refs. 75 and 76, it is pointed out that the interaction parameters have significant orbital dependence. In Ref. 75,

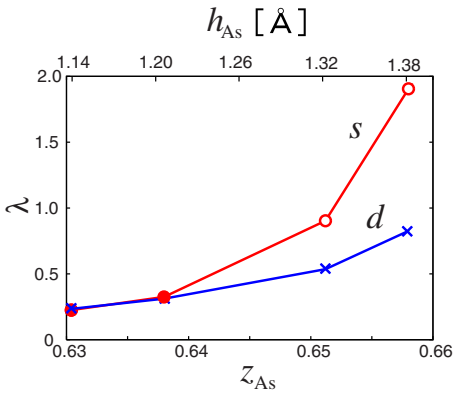

FIG. 9. (Color online) s-wave and d-wave eigenvalues of the Eliashberg equation plotted against z_{As} (lower scale) or h_{As} (upper scale) for $n=6.1$. The lattice constants are fixed at the original values for LaFeAsO. For the s wave, the open (solid) circles indicate that the gap is nodeless (nodal).

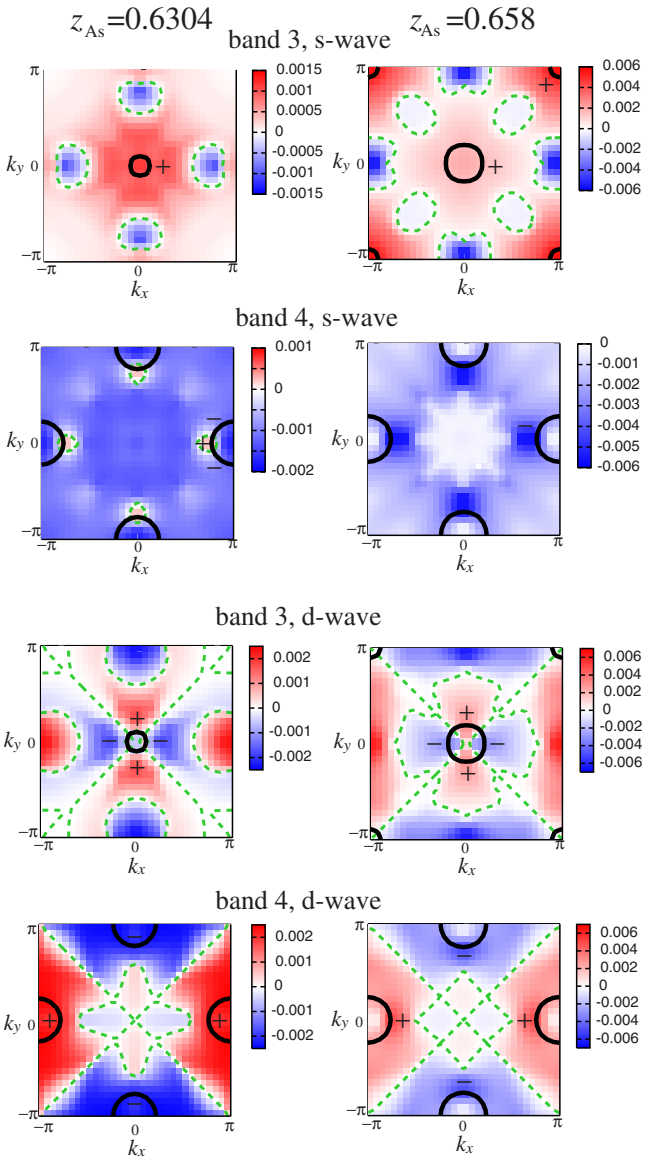

FIG. 10. (Color online) The gap functions for the model with z_{As}=0.6304 (left panels) or z_{As}=0.658 (right). From top to bottom: s wave in band 3, s wave in band 4, d wave in band 3, and d wave in band 4.

the intraorbital repulsions are U=3.27, 2.77, 2.20, and 3.31 (eV) for $d_{3Z^2-R^2}$, $d_{XZ/YZ}$, $d_{X^2-Y^2}$, and d_{XY} orbitals, respectively. This variation comes from the fact that each Fe 3d orbital hybridizes with As 4p quite differently. Namely, while the local basis of the five-band model, $\{d_i^\dagger\}$, can be represented as a linear combination of atomic $\tilde{d}^\dagger$ and $\tilde{p}^\dagger$ orbitals (as $\alpha_i\tilde{d}_i^\dagger+\Sigma_j\beta_{ij}\tilde{p}_j^\dagger$), the coefficients α_i, β_{ij} have a strong orbital dependence. For example, the ratio β_{ij}/α_i is large for $i=X^2-Y^2$ but small for, e.g., $i=3Z^2-R^2$. Therefore, if we adopt a common value for the interaction parameters for all five orbitals in the five-band model, electron correlations are relatively overestimated for X^2-Y^2, because $\tilde{p}$ orbitals are more weakly correlated than $\tilde{d}$ orbitals. In order to avoid this problem, we should use orbital-dependent interactions, where the interaction for $i=X^2-Y^2$ is small compared to others.

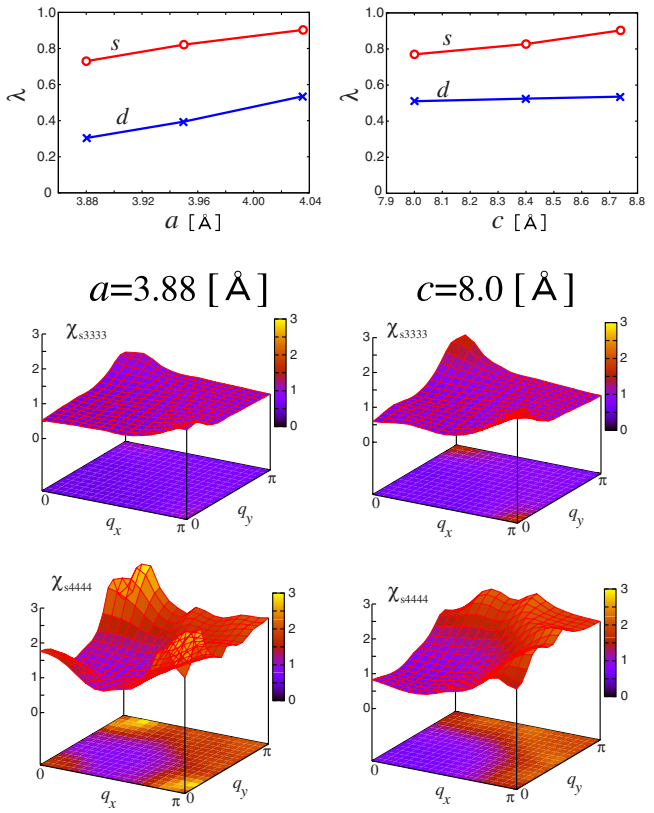

FIG. 11. (Color online) Upper panels: s-wave and d-wave eigenvalues of the Eliashberg equation plotted against a (left) or c (right), where h_{As} is fixed at the original value for LaFeAsO. Lower panels: χ_{s3333} and χ_{s4444} for a=3.88 Å with c fixed at the original value (left) and c=8.0 Å with a fixed at the original value (right).

So we study in this section the effect of the orbital dependence of the interactions, taking into account the orbital dependence of U', J, J' as well. Since the self-energy correction is not taken into account in RPA, it is again necessary to reduce the interactions to avoid magnetic ordering at high temperatures. Here we multiply all the interaction parameters in Ref. 75 by a factor of f=0.42, so the intraorbital interaction is taken to be 1.37, 1.16, 0.92, and 1.39 (eV) for $d_{3Z^2-R^2}$, $d_{XZ/YZ}$, $d_{X^2-Y^2}$, and d_{XY} orbitals, respectively. Since the $d_{X^2-Y^2}$ orbital has the smallest intraorbital interaction (0.92 eV in the present calculation as compared with 1.2 eV in the calculation for orbital-independent interactions), the effect of the $d_{X^2-Y^2}$ orbital is expected to be reduced compared with the results obtained by using the orbital-independent interactions.

First, we take the model for LaFeAsO to study the band-filling dependence. As shown in Fig. 12(a), we find that the s-wave pairing becomes nodal for $n>6.2$, i.e., the s wave becomes nodal for smaller electron doping compared to the case with orbital-independent interactions [see Fig. 6(a)]. Also, the nodal s-wave pairing still slightly dominates over d wave even at n=6.3, at which, for the case of orbital-independent interactions, the s gives way to d. If we turn to the pnictogen-height dependence of the eigenvalue of the Eliashberg equation in Fig. 12(b), the s wave is again enhanced with the increased height, but the enhancement is

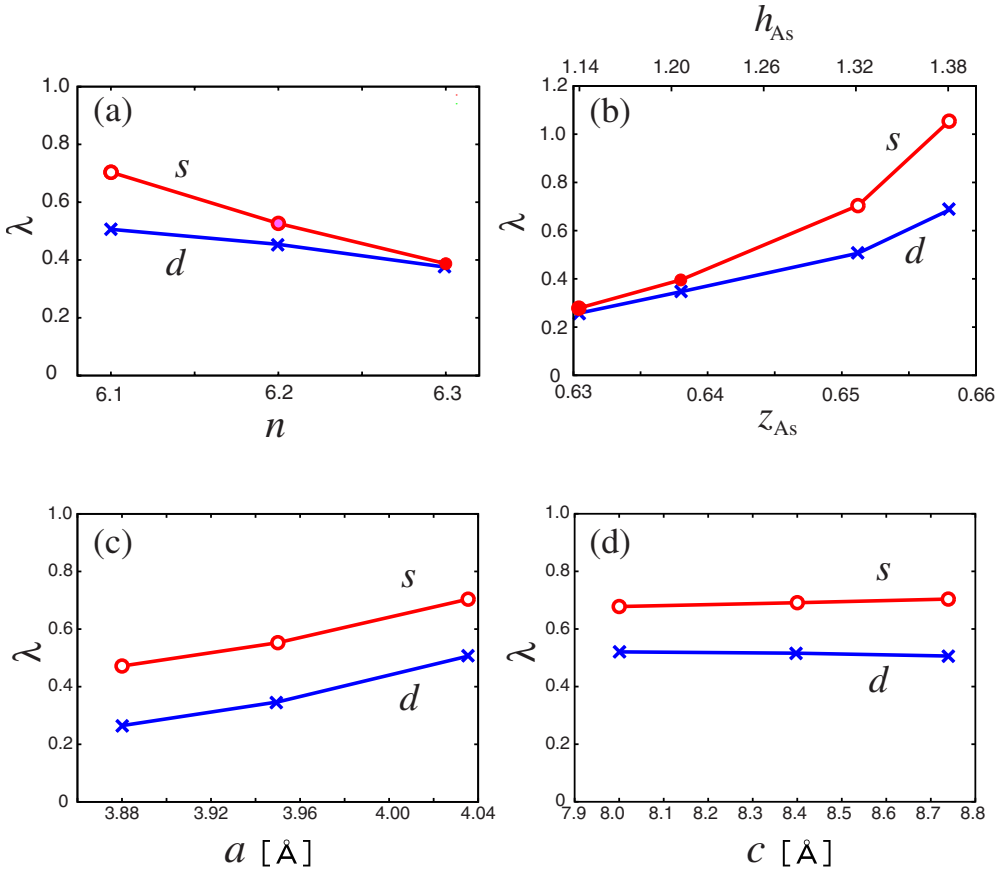

FIG. 12. (Color online) s-wave and d-wave eigenvalues of the Eliashberg equation calculated for orbital-dependent interactions, plotted against (a) n for the model of LaFeAsO, (b) z_{As} or h_{As} for $n=6.1$ with the lattice constants fixed at the original values for LaFeAsO, (c) a, and (d) c with h_{As} fixed at the original value for LaFeAsO. In (a), the light red (or gray) symbol for s wave at $n=6.2$ indicates that the gap is nearly nodal, while the red (or solid) symbol at $n=6.3$ stands for the nodal s wave.

smaller than in the case of Fig. 9, which can be attributed to the reduction in the γ (namely, the $d_{X^2-Y^2}$) Fermi-surface effect. As for the lattice-constant dependence depicted in Figs. 12(c) and 12(d), we find that the reduction in a suppresses λ, while that of c has small effect. This is because the reduction in c mainly enhances the $d_{X^2-Y^2}$ hopping, and the suppression of the electron correlation within this orbital has small effect when the intraorbital interaction is small.

Another effect of adopting orbital-dependent interactions appears in the symmetry of the gap function. For $z_{As}=0.658$ with $n=6.1$, we have seen that the gap is large at the $d_{X^2-Y^2}$ charactered portions of the Fermi surface when we adopt orbital-independent interactions. For the orbital-dependent interactions, the absolute value of the gap is nearly constant for each of the all pockets as shown in the left panel of Fig. 13(b) for band 4. This should be again because the magnitude of the gap is reduced at $d_{X^2-Y^2}$ portions of the Fermi surface due to the reduction in the $d_{X^2-Y^2}$ intraorbital interaction. The effect of reducing the $d_{X^2-Y^2}$ orbital interaction can be clearly seen in the comparison between χ_{s3333} and χ_{s4444} depicted in Fig. 13(c), where the two components have similar magnitudes for $z_{As}=0.658$ in contrast to the result for the orbital-independent interactions in Fig. 8(a).

VI. CALCULATION FOR ACTUAL MATERIALS

In this section, we calculate the band structure of actual materials other than LaFeAsO, i.e., the phosphate and Nd compound, using the experimentally determined lattice structure to construct the five-band model. The band filling will be fixed mainly at $n=6.1$ to make a direct comparison with the results for LaFeAsO. The results are interpreted in view of the general trend obtained in the study of the virtual lattice structures.

A. LaFePO

The band structure of the five-band model for LaFePO is shown in Fig. 14. In the case of LaFePO, the lattice constants are small compared to LaFeAsO (while closer to NdFeAsO below). However, the hopping integrals are similar to or larger than those for the virtual structure for LaFeAsO with $z_{As}=0.6304$. Thus, the main difference from LaFeAsO is caused by the height of P. The top of the $d_{X^2-Y^2}$ band at (π,π) is indeed pushed below the Fermi level,[69] and this makes the $(\pi,\pi/2)$ spin fluctuations arising from the β-β nesting dominate in χ_{s4444} as shown in Fig. 15.

This behavior in the spin fluctuation for LaFePO acts to make the d-wave pairing (Fig. 15, right) dominate for the

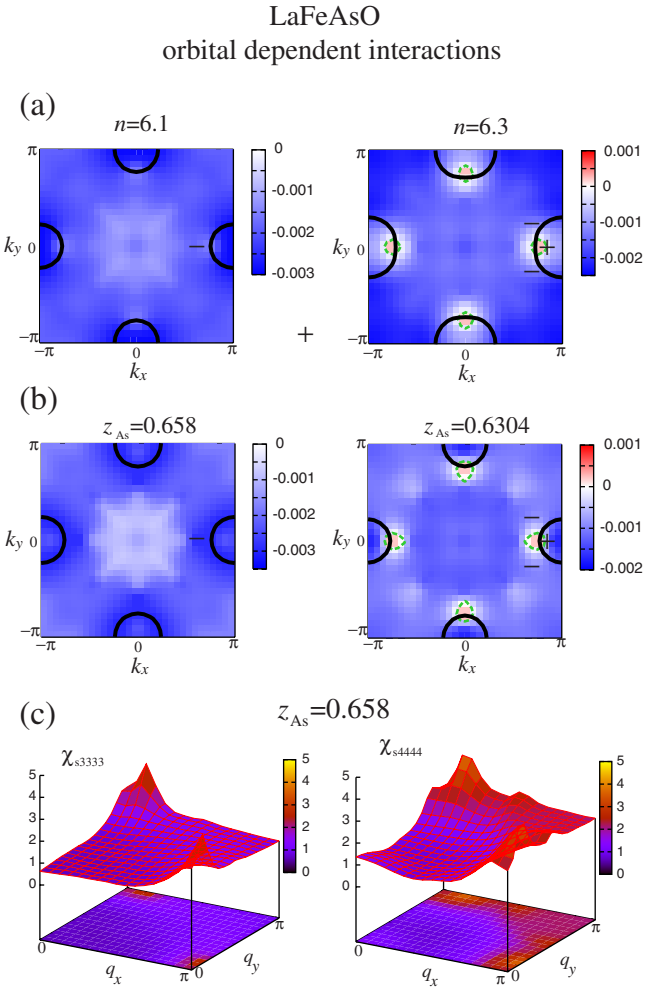

FIG. 13. (Color online) The gap function for band 4 calculated with the orbital-dependent interactions for (a) LaFeAsO with $n=6.1$ (left) and $n=6.3$ (right), and (b) $z_{\mathrm{As}}=0.658$ (left) and $z_{\mathrm{As}}=0.6304$ (right) with $n=6.1$. (c) χ_{s3333} and χ_{s4444} for $z_{\mathrm{As}}=0.658$ and $n=6.1$.

orbital-independent interactions, while the sign-reversing s wave with nodes intersecting the β Fermi surface (Fig. 15, left) is also closely competing. The U dependence of the eigenvalue of the Eliashberg equation is shown in Fig. 16(a). If we adopt the orbital-dependent interactions introduced in Sec. V C, on the other hand, we find that the nodal s wave slightly dominates over d wave in the entire parameter regime studied, as depicted in Fig. 16(b) for the eigenvalue of the Eliashberg equation against the interaction strength (i.e., the multiplication factor f here). This is expected from the comparison between Figs. 6(a) and 12(a), where we can see that the orbital-dependent interaction tends to favor nodal s wave over d wave.

We further find that the s-d competition depends on the band filling (not shown), i.e., smaller band fillings tend to favor the nodal s wave. As seen from these results the competition between nodal s-wave and d-wave pairings in LaFePO is rather subtle, and it is difficult to theoretically determine which symmetry actually takes place. In either case, however, superconducting gap of LaFePO is expected to have nodes intersecting the Fermi surface. This is in fact

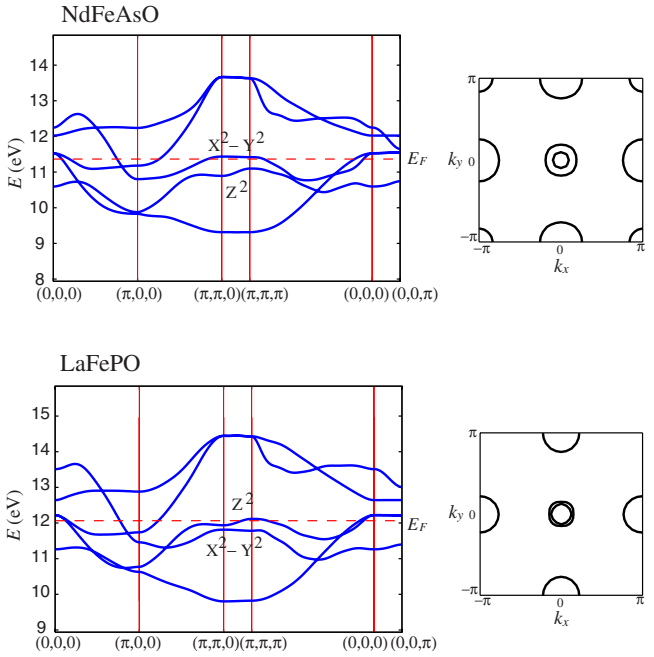

FIG. 14. (Color online) The band structure of the five-band model of the optimally doped NdFeAsO (upper panels) and LaFePO (lower). The Fermi surface at $k_z=0$ for $n=6.1$ is shown on the right.

consistent with recent experiments on LaFePO that suggest the presence of nodes in the superconducting gap.[58,59]

B. NdFeAsO

The band structure of NdFeAsO is shown in Fig. 14. The low-temperature lattice structure of the optimally doped sample (sample 4) in Ref. 50 is adopted here. Here, we have performed a local-density calculation (LDA) calculation with the plane-wave basis set using the pseudopotential of Nd obtained with the open-core treatment for the f electrons. The $d_{X^2-Y^2}$ band at (π,π) is seen to cross the Fermi level even at $n=6.1$ as expected, and the $(\pi,0)$ spin fluctuation strongly dominates in χ_{s4444} as shown in the right panel of Fig. 17(a), and the fully gapped sign-reversing s wave shown in Fig. 18(a) strongly dominates over d wave. For the orbital-independent interactions, the eigenvalue of the Eliashberg equation is $\lambda=1.20$ for s wave, which is indeed greater than that for LaFeAsO ($\lambda=0.90$), but not as large as the virtual lattice structure of LaFeAsO where the As height is increased to the value of NdFeAsO ($\lambda=1.91$). The latter property can mainly be attributed to the reduction in the lattice constants a and c in NdFeAsO as compared to those of LaFeAsO.

When we adopt the orbital-dependent interactions introduced in Sec. V C, the enhancement of λ from the LaFeAsO value is weaker than in the case of orbital-independent interactions, as expected from the previous discussion. Namely, $\lambda_{\mathrm{La}}=0.70$ and $\lambda_{\mathrm{Nd}}=0.72$ for the multiplication factor $f=0.42$ while $\lambda_{\mathrm{La}}=1.20$ and $\lambda_{\mathrm{Nd}}=1.32$ for $f=0.45$. The magnitude of the gap for the s-wave pairing is nearly constant on each of the all pockets as shown in Fig. 18(b), which is also expected from the argument in Sec. V C.

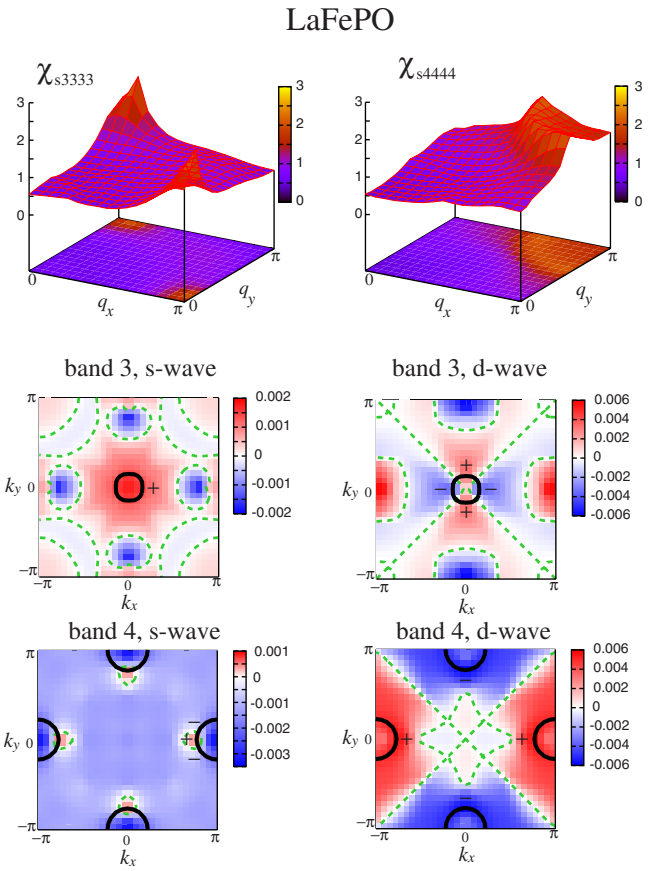

FIG. 15. (Color online) Upper panels: χ_{s3333} and χ_{s4444} for the five-band model for LaFePO with $n=6.1$, $U=1.7$, $U'=1.4$, and $J=J'=0.15$ (orbital-independent interactions). Lower panels: s-wave (left) and d-wave (right) gap functions for bands 3 and 4 for the same parameter values.

We have also performed a calculation for NdFeAsO with the lattice structure in the underdoped regime (sample 1 in Ref. 50). Here we take the band filling of $n=6.03$ and adopt orbital-independent interactions. As shown in Fig. 17, the maximum value of χ_{s4444} (and also χ_s, not shown) is larger than in the case of the optimally doped lattice structure because the nesting is better for the underdoped case. Nonetheless, the eigenvalue of the Eliashberg equation is found to be smaller, $\lambda=1.03$ for the s wave as compared to $\lambda=1.2$ for the optimally doped sample. This shows that removing the electrons to make the γ Fermi surface more effective does not necessarily favor superconductivity. This may be because lowering the Fermi level results in the decrease in the $d_{X^2-Y^2}$ density of states on the β Fermi surface, where the $d_{X^2-Y^2}$ band forms a Dirac cone. Doping the electrons raises the Fermi level, thereby increasing the $d_{X^2-Y^2}$ density of states on the β Fermi surface, and at the same time increasing the pnictogen height, which pushes up the $d_{X^2-Y^2}$ band at (π,π) so as to catch up with the raised Fermi level. The increased $d_{X^2-Y^2}$ density of states upon doping is seen in the broad $(\pi,0)$ peak structure in χ_{s4444} in the optimally doped case as compared to that in the underdoped regime (Fig. 17).

The tendency that electron doping tends to increase the pnictogen height should be general because the increase in the negative charge in the Fe layers suppresses the attractive

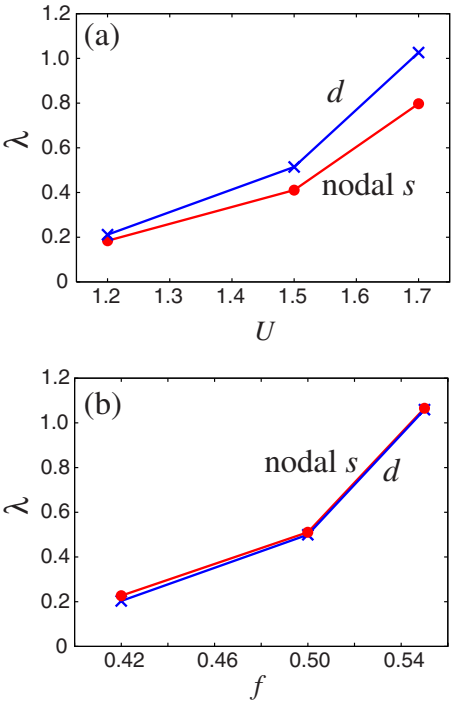

FIG. 16. (Color online) s-wave and d-wave eigenvalues of the Eliashberg equation for LaFePO plotted against (a) U with orbital-independent interactions with $U-U'=2J=0.3$ fixed, and (b) the multiplication factor f with orbital-dependent interactions. The s-wave gap here always has nodes intersecting the β Fermi surface.

interaction between the positively charged iron and the negatively charged pnictogen. Therefore, the doping dependence of λ shown in Fig. 6(a) with a fixed band structure may be too naive in that the effect of the γ Fermi surface monotonically decreases with the higher electron doping. As for the doping dependence of superconductivity, other than the ef-

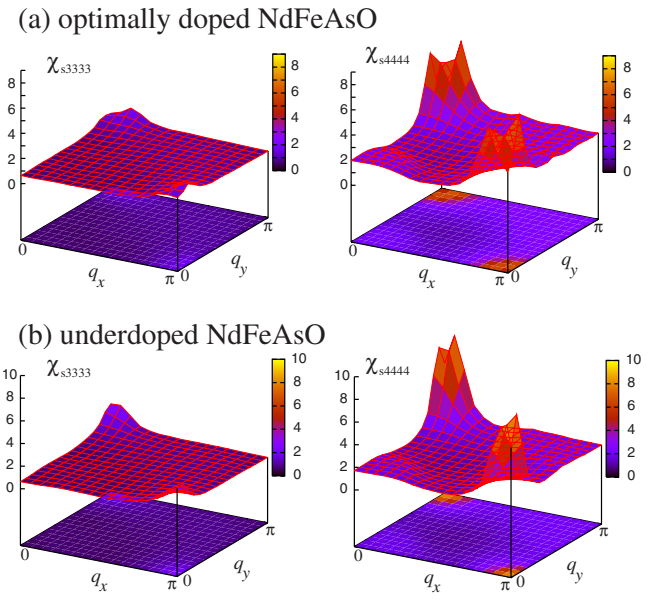

FIG. 17. (Color online) χ_{s3333} (left panels) and χ_{s4444} (right) in the five-band model for (a) the optimally doped NdFeAsO with $n=6.1$, and (b) the underdoped NdFeAsO with $n=6.03$.

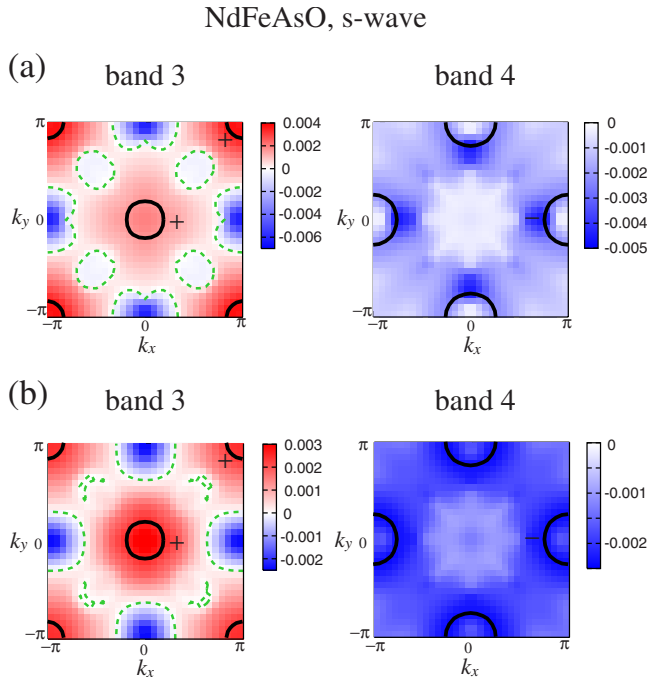

FIG. 18. (Color online) The *s*-wave gap function for band 3 (left panels) and band 4 (right) for the optimally doped NdFeAsO. Orbital-independent (a) and dependent (b) interactions are adopted.

fect of the change in the band structure, there have also been theoretical studies that suggest the importance of the "unscreening effect" of the Coulomb interaction,[82] or the importance of the electron correlation.[13]

We have finally examined the effect of pressure on NdFeAsO. The lattice structure data for $NdFeAsO_{1-y}$ under a pressure of 3.8 GPa is taken from Ref. 81. Applying pressure on NdFeAsO tends to reduce h_{As} as well as the lattice constants. At 3.8 GPa, the height is reduced to $h_{As}=1.33$ Å. This results in a suppression of the eigenvalue of the Eliashberg equation, and the *s*-wave eigenvalue is reduced regardless of the choice of the electron-electron interactions, e.g., for the orbital-independent interactions, λ at $T=0.02$ reduces (from 1.2) to 0.67. The suppression of λ is at least qualitatively consistent with the experiment.[57,83]

VII. DISCUSSIONS

A. Validity of the five-band model

One of the most important next steps in the microscopic study on superconductivity in the iron-based superconductors should be an examination of the present scenario based on the Fermi-surface nesting by means of self-consistent calculations. Indeed, if we are interested in the behavior of the present five-orbital (*d*-only) model with moderate (realistic) size of the Hund coupling[77] or the Coulomb interactions[75,76] estimated by various *ab initio* methods, we have obviously to take account of the self-energy (otherwise we have magnetic ordering at rather high temperatures), where the self-energy correction generally affects the effect of Fermi-surface nesting, which is usually overestimated in RPA.

One possible way to go beyond RPA is employing the fluctuation exchange (FLEX) approximation.[84] However, it has recently been recognized that FLEX does not work so successfully for the five-orbital model with moderate correlations. Namely, while we naively expect that the model should have a strong instability for the stripe-type antiferromagnetic ordering for undoped LaFeAsO, the spin susceptibility in FLEX has a peak at (π,π), which corresponds to the checkerboard-type antiferromagnetic instability. Even in the weakly correlated regime, Ikeda[13] had to introduce artificial level shifts for d_{z^2} and $d_{x^2-y^2}$ to the original LDA band in order to avoid a large d_{z^2} Fermi surface.

These problems seem to come from the fact that the self-energy correction generally has a strong orbital dependence in the five-orbital model rather than from some problems in FLEX. Even in the simple Hartree approximation for the paramagnetic case, the band structure and the Fermi surface dramatically change from those in LDA due to the Hartree field ($\sim U\langle n_i\rangle$) since the filling of each of the five orbitals varies so differently [e.g., $n\sim 0.8(0.5)$ for $d_{z^2}(d_{x^2-y^2})$].

On the other hand, in the *dpp* model that takes account of Fe 3*d* and As 4*p* and O 2*p* (Ref. 69) for which five Fe 3*d* orbitals are similarly filled, we do not have such problems as far as we introduce a gap (the so-called double-counting term Δ) that depends on the difference between the correlations in Fe 3*d* and As 4*p*.[85] In fact, this double-counting term in the *dpp* model makes the situation in the five-orbital model subtle. For the *dpp* model, we can safely assume that Δ does not have a serious orbital dependence. On the other hand, if we translate Δ in terms of the five-orbital model, we have to assume that Δ has a nontrivial orbital dependence since each Fe 3*d* hybridizes with As 4*p* differently (e.g., while the hybridization between $d_{x^2-y^2}$ and As 4*p* is strong, those between d_{z^2} and As 4*p* are weak[69]). This should be one reason why Ikeda had to introduce an orbital-dependent level shift in his FLEX calculation.[13]

Therefore, we believe that it is impossible to obtain any meaningful results in self-consistent calculation for the five-orbital model without considering the orbital-dependent double-counting term, while we have still no guarantee that the double-counting term can really make the five-orbital model mimic the original *dpp* model. An interesting observation is that the situation is in sharp contrast with the case of high-T_c cuprates. For cuprates, aside from the issue of the validity of the single-band Hubbard model or the *t*-*J* model, we can naively expect that the self-consistent solutions of these models can at least describe Mott insulator, metallic state with strong antiferromagnetic fluctuations, etc. On the other hand, for iron pnictides we have to seriously examine whether the five-orbital model indeed has a self-consistent solution with the stripe-type antiferromagnetic instability. This is why we consider this an important future problem.

B. Phase diagram

In the preceding sections, it has been shown that the pnictogen height can act as a switch between high-T_c nodeless and low-T_c nodal superconductivities. We have also shown that the increase in the lattice constants is unfavorable for

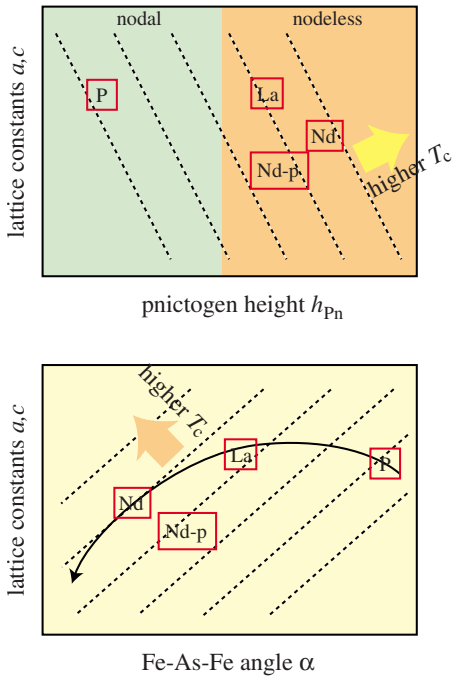

FIG. 19. (Color online) Schematic superconducting phase diagram on the h_{Pn}-[a,c] (upper) and α-[a,c] (lower) planes. The dashed lines are schematic contours of T_c. The curved arrow in the lower panel schematically indicates how the lattice parameters vary as the bond angle α is decreased in Ref. 50. The shorthands for materials are the same as in Table I.

superconductivity. These tendencies can be incorporated in a schematic phase diagram shown in Fig. 19. In the upper panel, we take the pnictogen height as the horizontal axis, and lattice constants as the vertical axis. In LnFeAsO, the lattice constants decrease monotonically in the chemical trend La→Nd→Dy.[52] On the other hand, the As height monotonically increases, and these effects may cancel with each other to result in a nearly constant T_c between Ln=Nd and Dy.[52] In the lower panel of Fig. 19, we adopt the As-Fe-As bond angle α as the horizontal axis to make clear comparison with Ref. 50, in which it was shown that the maximum T_c seems to be reached when the pnictogens form a regular tetrahedron. As schematically indicated by a curved arrow, the appearance of the maximum T_c may be a consequence of the combined effect of the bond angle and the lattice constants. Thus, as far as the present theoretical study is concerned, the pnictogen height is a better parameter than the angle α to draw a phase diagram since α is affected by both the height and the lattice constant a, which have opposite effects on T_c.

To attain higher T_c on the basis of this phase diagram, it is desirable to have higher position of the pnictogen while keeping lattice constants not reduced. On the other hand, we have to keep in mind that such a variation in the lattice parameters also enhances the tendency toward magnetism. Experimentally, magnetic ordering is known to occur after the structural phase transition, and the tendency toward magnetism and the structural phase transition seem to be linked. In this sense, the superconductivity will have to compete with the magnetism/structural phase transition in a more severe manner as the height and/or the lattice constants are increased. Namely, too much increase in the height and/or the lattice constants can be unfavorable for superconductivity in that the magnetism/structural phase transition, which may take place at high temperatures, can dominate over superconductivity. In such a case, applying pressure to reduce the lattice constants and/or doping carriers can be effective to suppress the magnetism or the structural phase transition. This seems to be the case for the undoped LaFeAsO (Ref. 86) and $CaFe_2As_2$,[87] where structural phase transition and magnetism take place at ambient pressure, while applying pressure seems to remove the phase transition to result in superconductivity. A better understanding of the competition between superconductivity and magnetism should require further understanding of the magnetic state sitting next to the superconducting state. Namely, the mutual relation among the so-called "spin-density wave" state observed experimentally,[88,89] the magnetic state obtained in first-principles calculations,[88,90–92] and the spin fluctuation obtained in the downfolded five-band models has to be made clearer.

Another point that should be kept in mind is the material dependence of the electron-electron interactions, which is not considered in the present phase diagram. In particular, the difference in the lattice structure in the 11 systems such as FeSe (Ref. 93) and in the hole-doped 122 systems such as $BaFe_2As_2$ (Ref. 94) can affect the effective electron-electron interaction within the FeAs planes. Also, the screening effect of the f orbitals may be different between LaFeAsO and NdFeAsO. On the f electrons, the present analysis adopts open-core treatment for the f electrons of Nd, whose validity may have to be examined. We cannot completely rule out the possibility that the hybridization between Nd f and Fe d electrons can affect the electronic states and thus the superconductivity. In these senses, the actual phase diagram for the entire family of the iron-based superconductors should have more axes than presented here.

VIII. CONCLUSION

In the present study, we have investigated how the lattice structure affects the spin-fluctuation mediated superconductivity in iron pnictides. The obtained picture is that the gap function and T_c are determined by the competition or cooperation of the multiple spin-fluctuation modes arising from α-β, β_1-β_2, and γ-β Fermi-surface nestings, which depend on the materials, band filling, and/or pressure. In particular, the competition between β_1-β_2 and γ-β nestings within portions of the Fermi surface having strong $d_{X^2-Y^2}$ character governs the form of the superconducting gap as well as the strength of the superconducting instability. The relevance of the γ (quasi) Fermi surface is determined by the pnictogen height, and consequently, the pnictogen height plays the role of a switch between high-T_c nodeless and low-T_c nodal pairings, which may give the answer to the question of why the form of the superconducting gap, as well as T_c are vastly different between LaFeAsO and LaFePO.[58,59] An intriguing observation is, since d wave and the nodal s wave tend to be closely competing for low pnictogen heights, there is a pos-

sibility of exotic pairing such as $s+id$.[95] The lattice constant also affects superconductivity in the manner that the reduction in a (c) mainly suppresses the electron correlation within d_{XZ}/d_{YZ} ($d_{X^2-Y^2}$) orbitals and thus degrades superconductivity. A schematic phase diagram has been obtained by combining the effect of the pnictogen height and the lattice constants.

The low T_c in cases where the β_1-β_2 nesting dominates over γ-β nesting can be naturally understood in the sense that there is a kind of frustration between β_1-β_2, α-β_1, and α-β_2 nestings in determining the form of the gap because the sign of the gap has to be changed across each of the multiple nesting vectors (see Fig. 4). Conversely, the high T_c in the case where the γ-β nesting, along with α-β, dominates over β_1-β_2 is natural in that the unfrustrated gap fully opens on all five disconnected pieces of the Fermi surface, α_1, α_2, β_1, β_2, and γ. In this sense, high T_c in iron pnictides can be understood as a realization of the theoretical proposal that one can look for high-T_c superconductors in systems with disconnected Fermi surfaces.[96,97]

The form of the s-wave gap is shown to be nonuniversal, even when the gap is fully open, and its variation along the Fermi surface strongly depends on the band structure (i.e., the lattice structure), the band filling, and the electron-electron interactions. When the s-wave gap varies significantly along the Fermi surface, it is also expected to be affected by the presence of the impurities, as pointed out by Mishra *et al.*[28] In this sense, the form of the gap should experimentally be determined by a combination of multiple experiments on the same material, desirably on the same sample. From this viewpoint, the discrepancy between the NMR experiments for LaFeAsO and other experiments suggesting nearly isotropic gap may be a consequence of the nonuniversality of the superconducting gap, especially because LaFeAsO lies close to the nodeless/nodal boundary. In fact, anisotropic $s\pm$wave pairing where the gap varies strongly on the β Fermi surface has been proposed to explain the T^3 decay in the NMR experiment.[98] This view may also give some clue as to why some of the tunneling spectroscopy measurements exhibit zero-bias conductivity peak,[99] which is an indication of unconventional sign-reversing pairing,[100] while others do not.[101] It is worth noting that recent theoretical studies show that it is unlikely to observe the zero-bias conductivity peak for the fully gapped sign-reversing s-wave pairing.[102,103]

In the present study, we have focused on the LnFeAsO (1111) systems. In the 11 systems such as FeSe, experiments under pressure also suggest strong structure dependence of superconductivity.[104–107] However, there may be some discrepancies from the 1111 systems regarding the lattice structure dependence since the LnO layer is not present. Also, the extremely high position of the chalcogen atom in 11 systems [1.47 Å in FeSe (Ref. 108) and 1.76 Å in FeTe (Ref. 109)] may affect the lattice structure dependence. Our study focusing on the 11 systems is now underway. Similarly, the hole-doped 122 systems are also expected to have some discrepancies with the electron-doped 1111 systems, which also deserve future study.

ACKNOWLEDGMENTS

We wish to thank H. Eisaki, T. Ito, C.-H. Lee, R. Kumai, and N. Takeshita for valuable discussions on the correlation between the lattice structure and T_c, and also providing some of the lattice structure data prior to publication. We also thank Y. Tanaka and H. Kontani for valuable discussions. R.A. would like to thank K. Nakamura, M. Imada, A. Toschi, P. Hansmann, G. Sangiovanni, K. Held, Z. Pchelkina, I. Solovyev, and H. Ikeda for fruitful discussion on the validity of the five-band model. Numerical calculations were performed at the facilities of the Information Technology Center, University of Tokyo, and also at the Supercomputer Center, ISSP, University of Tokyo. This study has been supported by Grants-in-Aid for Scientific Research from MEXT of Japan and from the Japan Society for the Promotion of Science. H.U. acknowledges support by the Japan Society for the Promotion of Science.

[1] Y. Kamihara, T. Watanabe, M. Hirano, and H. Hosono, J. Am. Chem. Soc. **130**, 3296 (2008).
[2] Z.-A. Ren, W. Lu, J. Yang, W. Yi, X.-L. Shen, Z.-C. Li, G.-C. Che, X.-L. Dong, L.-L. Sun, F. Zhou, and Z.-X. Zhao, Chin. Phys. Lett. **25**, 2215 (2008).
[3] L. Boeri, O. V. Dolgov, and A. A. Golubov, Phys. Rev. Lett. **101**, 026403 (2008).
[4] I. I. Mazin, D. J. Singh, M. D. Johannes, and M. H. Du, Phys. Rev. Lett. **101**, 057003 (2008).
[5] K. Kuroki, S. Onari, R. Arita, H. Usui, Y. Tanaka, H. Kontani, and H. Aoki, Phys. Rev. Lett. **101**, 087004 (2008).
[6] I. Mazin and J. Schmalian, Physica C **469**, 614 (2009).
[7] K. Kuroki, S. Onari, R. Arita, H. Usui, Y. Tanaka, H. Kontani, and H. Aoki, Phys. Rev. Lett. **102**, 109902(E) (2009): in Ref. 5, the gap function (diagonal element) of the fourth band had nodes intersecting the β Fermi surface. This was in fact due to a technical error in the final stage of the calculation, i.e., the unitary transformation from the orbital to the band representations. However, the main conclusions of Ref. 5 do remain unaltered since (i) the magnitude of the gap along the β Fermi surface varies significantly as mentioned in the present study and (ii) the coexistence of $(\pi,\pi/2)$ and $(\pi,0)$ spin fluctuations determines the way in which nodes appear as also shown in the present study. In Ref. 5, the importance of the off-diagonal elements in the band representation was pointed out in that they open up a full gap on the Fermi surface even when there are nodes in the diagonal elements. However, since the five bands are apart by at least O (0.1 eV) in most of the portions, the off-diagonal elements in the band representation, which should be much smaller than 0.1 eV, is generally irrelevant as far as the quasiparticle excitation is concerned. In special cases where several bands sit close to each other near the Fermi level, the off-diagonal elements may become relevant.
[8] X. Qi, S. Raghu, C. Liu, D. Scalapino, and S. Zhang, arXiv:0804.4332 (unpublished).
[9] S. Raghu, X.-L. Qi, C.-X. Liu, D. J. Scalapino, and S.-C. Zhang, Phys. Rev. B **77**, 220503(R) (2008).
[10] M. Daghofer, A. Moreo, J. A. Riera, E. Arrigoni, D. J. Scalapino, and E. Dagotto, Phys. Rev. Lett. **101**, 237004 (2008).
[11] A. V. Chubukov, D. V. Efremov, and I. Eremin, Phys. Rev. B **78**,

134512 (2008).
[12] T. Nomura, J. Phys. Soc. Jpn. **77**, Suppl. C 123 (2008).
[13] H. Ikeda, J. Phys. Soc. Jpn. **77**, 123707 (2008).
[14] F. Wang, H. Zhai, Y. Ran, A. Vishwanath, and D.-H. Lee, Phys. Rev. Lett. **102**, 047005 (2009).
[15] Z. Yao, J. Li, and Z. Wang, New J. Phys. **11**, 025009 (2009).
[16] S.-L. Yu, J. Kang, and J.-X. Li, Phys. Rev. B **79**, 064517 (2009).
[17] Y. Yanagi, Y. Yamakawa, and Y. Ono, J. Phys. Soc. Jpn. **77**, 123701 (2008).
[18] V. Cvetkovic and Z. Tesanovic, EPL **85**, 37002 (2009).
[19] R. Arita, S. Onari, H. Usui, K. Kuroki, Y. Tanaka, H. Kontani, and H. Aoki, J. Phys.: Conf. Ser. **150**, 052010 (2009).
[20] K. Kuroki, S. Onari, R. Arita, H. Usui, Y. Tanaka, H. Kontani, and H. Aoki, New J. Phys. **11**, 025017 (2009).
[21] K. Kuroki and H. Aoki, Physica C **469**, 635 (2009).
[22] T. Kariyado and M. Ogata, J. Phys. Soc. Jpn. **78**, 043708 (2009).
[23] M. Ishikado, R. Kajimoto, S. Shamoto, M. Arai, A. Iyo, K. Miyazawa, P. M. Shirage, H. Kito, H. Eisaki, S. Kim, H. Hosono, T. Guidi, R. Bewley, and S. M. Bennington, J. Phys. Soc. Jpn. **78**, 043705 (2009).
[24] K. Matan, R. Morinaga, K. Iida, and T. J. Sato, Phys. Rev. B **79**, 054526 (2009).
[25] S. Graser, T. A. Maier, P. J. Hirschfeld, and D. J. Scalapino, New J. Phys. **11**, 025016 (2009).
[26] T. Maier, S. Graser, D. Scalapino, and P. Hirschfeld, arXiv:0903.5216 (unpublished).
[27] C. Cao, P. J. Hirschfeld, and H.-P. Cheng, Phys. Rev. B **77**, 220506(R) (2008).
[28] V. Mishra, G. Boyd, S. Graser, T. Maier, P. J. Hirschfeld, and D. J. Scalapino, Phys. Rev. B **79**, 094512 (2009).
[29] K. Seo, B. A. Bernevig, and J. Hu, Phys. Rev. Lett. **101**, 206404 (2008).
[30] H. Ding, P. Richard, K. Nakayama, T. Sugawara, T. Arakane, Y. Sekiba, A. Takayama, S. Souma, T. Sato, T. Takahashi, Z. Wang, X. Dai, Z. Fang, G. F. Chen, J. L. Luo, and N. L. Wang, EPL **83**, 47001 (2008).
[31] K. Nakayama, T. Sato, P. Richard, Y. Xu, Y. Sekiba, S. Souma, G. Chen, J. Luo, N. Wang, H. Ding, and T. Takahashi, EPL **85**, 67002 (2009).
[32] K. Hashimoto, T. Shibauchi, T. Kato, K. Ikada, R. Okazaki, H. Shishido, M. Ishikado, H. Kito, A. Iyo, H. Eisaki, S. Shamoto, and Y. Matsuda, Phys. Rev. Lett. **102**, 017002 (2009).
[33] H. Luetkens, H.-H. Klauss, R. Khasanov, A. Amato, R. Klingeler, I. Hellmann, N. Leps, A. Kondrat, C. Hess, A. Kohler, G. Behr, J. Werner, and B. Buchner, Phys. Rev. Lett. **101**, 097009 (2008).
[34] A. A. Aczel, E. Baggio-Saitovitch, S. L. Budko, P. C. Canfield, J. P. Carlo, G. F. Chen, Pengcheng Dai, T. Goko, W. Z. Hu, G. M. Luke, J. L. Luo, N. Ni, D. R. Sanchez-Candela, F. F. Tafti, N. L. Wang, T. J. Williams, W. Yu, and Y. J. Uemura, Phys. Rev. B **78**, 214503 (2008).
[35] T. Goko, A. Aczel, E. Baggio-Saitovitch, S. Bud'ko, P. Canfield, J. Carlo, G. Chen, P. Dai, A. Hamann, W. Hu, H. Kageyama, G. Luke, J. Luo, B. Nachumi, N. Ni, D. Reznik, D. Sanchez-Candela, A. Savici, K. Sikes, N. Wang, C. Wiebe, T. Williams, T. Yamamoto, W. Yu, and Y. Uemura, arXiv:0808.1425 (unpublished).
[36] M. Hiraishi, R. Kadono, S. Takeshita, M. Miyazaki, A. Koda, H. Okabe, and J. Akimitsu, J. Phys. Soc. Jpn. **78**, 023710 (2009).
[37] A. D. Christianson, E. A. Goremychkin, R. Osborn, S. Rosenkranz, M. D. Lumsden, C. D. Malliakas, I. S. Todorov, H. Claus, D. Y. Chung, M. G. Kanatzidis, R. I. Bewley, and T. Guidi, Nature (London) **456**, 930 (2008).
[38] M. D. Lumsden, A. D. Christianson, D. Parshall, M. B. Stone, S. E. Nagler, G. J. MacDougall, H. A. Mook, K. Lokshin, T. Egami, D. L. Abernathy, E. A. Goremychkin, R. Osborn, M. A. McGuire, A. S. Sefat, R. Jin, B. C. Sales, and D. Mandrus, Phys. Rev. Lett. **102**, 107005 (2009).
[39] T. A. Maier and D. J. Scalapino, Phys. Rev. B **78**, 020514(R) (2008).
[40] T. Maier, S. Graser, D. Scalapino, and P. Hirschfeld, arXiv:0903.0008 (unpublished).
[41] S. Onari and H. Kontani (private communication).
[42] A. Kawabata, S. C. Lee, T. Moyoshi, Y. Kobayashi, and M. Sato, J. Phys. Soc. Jpn. **77**, 103704 (2008).
[43] A. S. Sefat, A. Huq, M. A. McGuire, R. Jin, B. C. Sales, D. Mandrus, L. M. D. Cranswick, P. W. Stephens, and K. H. Stone, Phys. Rev. B **78**, 104505 (2008).
[44] A. S. Sefat, R. Jin, M. A. McGuire, B. C. Sales, D. J. Singh, and D. Mandrus, Phys. Rev. Lett. **101**, 117004 (2008).
[45] S. Matsuishi, Y. Inoue, T. Nomura, H. Yanagi, M. Hirano, and H. Hosono, J. Am. Chem. Soc. **130**, 14428 (2008).
[46] D. Parker, O. V. Dolgov, M. M. Korshunov, A. A. Golubov, and I. I. Mazin, Phys. Rev. B **78**, 134524 (2008).
[47] Y. Senga and H. Kontani, J. Phys. Soc. Jpn. **77**, 113710 (2008).
[48] Y. Senga and H. Kontani, New J. Phys. **11**, 035005 (2009).
[49] Y. Kamihara, H. Hiramatsu, M. Hirano, R. Kawamura, H. Yanagi, T. Kamiya, and H. Hosono, J. Am. Chem. Soc. **128**, 10012 (2006).
[50] C.-H. Lee, A. Iyo, H. Eisaki, H. Kito, M. T. Fernandez-Diaz, T. Ito, K. Kihou, H. Matsuhata, M. Braden, and K. Yamada, J. Phys. Soc. Jpn. **77**, 083704 (2008).
[51] J. Zhao, Q. Huang, C. de la Cruz, S. Li, J. W. Lynn, Y. Chen, M. A. Green, G. F. Chen, G. Li, Z. Li, J. L. Luo, N. L. Wang, and P. Dai, Nature Mater. **7**, 953 (2008).
[52] K. Miyazawa, K. Kihou, P. M. Shirage, C.-H. Lee, H. Kito, H. Eisaki, and A. Iyo, J. Phys. Soc. Jpn. **78**, 034712 (2009).
[53] H. Takahashi, K. Igawa, K. Arii, Y. Kamihara, M. Hirano, and H. Hosono, Nature (London) **453**, 376 (2008).
[54] K. Tatsumi, N. Fujiwara, H. Okada, H. Takahashi, Y. Kamihara, M. Hirano, and H. Hosono, J. Phys. Soc. Jpn. **78**, 023709 (2009).
[55] H. Okada, K. Igawa, H. Takahashi, Y. Kamihara, M. Hirano, H. Hosono, K. Matsubayashi, and Y. Uwatoko, J. Phys. Soc. Jpn. **77**, 113712 (2008).
[56] N. Takeshita (private communication).
[57] N. Takeshita, A. Iyo, H. Eisaki, H. Kito, and T. Ito, J. Phys. Soc. Jpn. **77**, 075003 (2008).
[58] J. D. Fletcher, A. Serafin, L. Malone, J. G. Analytis, J.-H. Chu, A. S. Erickson, I. R. Fisher, and A. Carrington, Phys. Rev. Lett. **102**, 147001 (2009).
[59] C. Hicks, T. Lippman, M. Huber, J. Analytis, J. Chu, A. Erickson, I. Fisher, and K. Moler, arXiv:0903.5260 (unpublished).
[60] Y. Nakai, K. Ishida, Y. Kamihara, M. Hirano, and H. Hosono, J. Phys. Soc. Jpn. **77**, 073701 (2008).
[61] N. Terasaki, H. Mukuda, M. Yashima, Y. Kitaoka, K. Miyazawa, P. M. Shirage, H. Kito, H. Eisaki, and A. Iyo, J. Phys. Soc. Jpn. **78**, 013701 (2009).
[62] K. Ahilan, F. L. Ning, T. Imai, A. S. Sefat, R. Jin, M. A. McGuire, B. C. Sales, D. Mandrus, Phys. Rev. B **78**, 100501(R)

(2008).
[63] K. Matano, Z. A. Ren, X. L. Dong, L. L. Sun, Z. X. Zhao, and Guo-qing Zheng, EPL **83**, 57001 (2008).
[64] H. Kotegawa, S. Masaki, Y. Awai, H. Tou, Y. Mizuguchi, and Y. Takano, J. Phys. Soc. Jpn. **77**, 113703 (2008).
[65] H. Fukazawa, T. Yamazaki, K. Kondo, Y. Kohori, N. Takeshita, P. M. Shirage, K. Kihou, K. Miyazawa, H. Kito, H. Eisaki, and A. Iyo, J. Phys. Soc. Jpn. **78**, 033704 (2009).
[66] Y. Kobayashi, A. Kawabata, S. Lee, T. Moyoshi, and M. Sato, arXiv:0901.2830 (unpublished).
[67] Y. Nakai, K. Ishida, Y. Kamihara, M. Hirano, and H. Hosono, Phys. Rev. Lett. **101**, 077006 (2008).
[68] D. J. Singh and M. H. Du, Phys. Rev. Lett. **100**, 237003 (2008).
[69] V. Vildosola, L. Pourovskii, R. Arita, S. Biermann, and A. Georges, Phys. Rev. B **78**, 064518 (2008).
[70] S. Lebegue, Z. P. Yin, and W. E. Pickett, New J. Phys. **11**, 025004 (2009).
[71] L. Zhang, A. Subedi, D. J. Singh, and M.-H. Du, Phys. Rev. B **78**, 174520 (2008).
[72] S. Baroni, A. Dal Corso, S. de Gironcoli, P. Giannozzi, C. Cavazzoni, G. Ballabio, S. Scandolo, G. Chiarotti, P. Focher, A. Pasquarello, K. Laasonen, A. Trave, R. Car, N. Marzari, and A. Kokalj (http://www.pwscf.org/); Here we adopt the exchange-correlation functional introduced by J. P. Perdew, K. Burke, and Y. Wang, Phys. Rev. B **54**, 16533 (1996), and the wave functions are expanded by plane waves up to a cutoff energy of 40 Ry 10^3 k-point meshes are used with the special points technique by H. J. Monkhorst and J. D. Pack, *ibid.* **13**, 5188 (1976).
[73] N. Marzari and D. Vanderbilt, Phys. Rev. B **56**, 12847 (1997); I. Souza, N. Marzari, and D. Vanderbilt, *ibid.* **65**, 035109 (2001); The Wannier functions are generated by the code developed by A. A. Mostofi, J. R. Yates, N. Marzari, I. Souza, and D. Vanderbilt (http://www.wannier.org/).
[74] H. Fukuyama, J. Phys. Soc. Jpn., Online News and Comments [May 12, 2008].
[75] K. Nakamura, R. Arita, and M. Imada, J. Phys. Soc. Jpn. **77**, 093711 (2008).
[76] T. Miyake, L. Pourovskii, V. Vildosola, S. Biermann, and A. Georges, J. Phys. Soc. Jpn. **77**, Suppl. C 99 (2008).
[77] V. Anisimov, Dm. M. Korotin, M. Korotin, A. Kozhevnikov, J. Kunes, A. Shorikov, S. Skornyakov, and S. Streltsov, J. Phys.: Condens. Matter **21**, 075602 (2009).
[78] K. Yada and H. Kontani, J. Phys. Soc. Jpn. **74**, 2161 (2005).
[79] T. Takimoto, T. Hotta, and K. Ueda, Phys. Rev. B **69**, 104504 (2004).
[80] Although the β_1 and β_2 Fermi surfaces are nearly circles centered around $(\pi,0)$ and $(0,\pi)$, the nesting vector is not (π,π) since a nesting vector relevant to spin fluctuations has to connect electrons and holes so that they are as depicted in Fig. 4.
[81] R. Kumai, N. Takashita, T. Ito, H. Kito, A. Iyo, and H. Eisaki, J. Phys. Soc. Jpn. **78**, 013705 (2009).
[82] Y. Fuseya, T. Kariyado, and M. Ogata, J. Phys. Soc. Jpn. **78**, 023703 (2009).
[83] The suppression of λ from 1.20 (ambient pressure) to 0.67 (3.8 GPa) seems to be too large considering that T_c=45 K at 3.8 GPa experimentally (Ref. 57). This may be because the lattice structure under pressure is determined at room temperature (Ref. 81), while we adopt the low-temperature lattice structure for ambient pressure (Ref. 50). In fact, it is found in Ref. 50 that h_{As} increases upon lowering the temperature for $NdFeAsO_{1-y}$.
[84] N. E. Bickers, D. J. Scalapino, and S. R. White, Phys. Rev. Lett. **62**, 961 (1989).
[85] T. Mizokawa, T. Sudayama, and Y. Wakisaka, J. Phys. Soc. Jpn. **77**, Suppl. C 158 (2009).
[86] H. Okada, K. Igawa, H. Takahashi, Y. Kamihara, M. Hirano, H. Hosono, K. Matsubayashi, and Y. Uwatoko, J. Phys. Soc. Jpn. **77**, 113712 (2008).
[87] M. S. Torikachvili, S. L. Bud'ko, N. Ni, and P. C. Canfield, Phys. Rev. Lett. **101**, 057006 (2008).
[88] J. Dong, H. J. Zhang, G. Xu, Z. Li, W. Z. Hu, D. Wu, G. F. Chen, X. Dai, J. L. Luo, Z. Fang, and N. L. Wang, EPL **83**, 27006 (2008).
[89] C. de la Cruz, Q. Huang, J. W. Lynn, Jiying Li, W. Ratcliff II, J. L. Zarestky, H. A. Mook, G. F. Chen, J. L. Luo, N. L. Wang, and P. Dai, Nature (London) **453**, 899 (2008).
[90] I. I. Mazin, M. D. Johannes, L. Boeri, K. Koepernik, and D. J. Singh, Phys. Rev. B **78**, 085104 (2008).
[91] S. Ishibashi, K. Terakura, and H. Hosono, J. Phys. Soc. Jpn. **77**, 053709 (2008).
[92] T. Yildirim, Phys. Rev. Lett. **101**, 057010 (2008).
[93] F.-C. Hsu, J.-Y. Luo, K.-W. Yeh, T.-K. Chen, T.-W. Huang, P. M. Wu, Y.-C. Lee, Y.-L. Huang, Y.-Y. Chu, D.-C. Yan, and M.-K. Wu, Proc. Natl. Acad. Sci. U.S.A. **105**, 14262 (2008).
[94] M. Rotter, M. Tegel, and D. Johrendt, Phys. Rev. Lett. **101**, 107006 (2008).
[95] W. Lee, S. Zhang, and C. Wu, Phys. Rev. Lett. **102**, 217002 (2009).
[96] K. Kuroki and R. Arita, Phys. Rev. B **64**, 024501 (2001).
[97] K. Kuroki, T. Kimura, and R. Arita, Phys. Rev. B **66**, 184508 (2002).
[98] Y. Nagai, N. Hayashi, N. Nakai, H. Nakamura, M. Okumura, and M. Machida, New J. Phys. **10**, 103026 (2008).
[99] L. Shan, Y. Wang, X. Zhu, G. Mu, L. Fang, C. Ren, and H.-H. Wen, EPL **83**, 57004 (2008).
[100] S. Kashiwaya and Y. Tanaka, Rep. Prog. Phys. **63**, 1641 (2000).
[101] T. Y. Chen, Z. Tesanovic, R. H. Liu, X. H. Chen, and C. L. Chien, Nature (London) **453**, 1224 (2008).
[102] A. Golubov, A. Brinkman, O. Dolgov, I. Mazin, and Y. Tanaka, arXiv:0812.5057 (unpublished).
[103] S. Onari and Y. Tanaka, Phys. Rev. B **79**, 174526 (2009).
[104] Y. Mizuguchi, F. Tomioka, S. Tsuda, T. Yamaguchi, and Y. Takano, Appl. Phys. Lett. **93**, 152505 (2008).
[105] S. Margadonna, Y. Takabayashi, Y. Ohishi, Y. Mizuguchi, Y. Takano, T. Kagayama, T. Nakagawa, M. Takata, and K. Prassides, arXiv:0903.2204 (unpublished).
[106] S. Medvedev, T. McQueen, I. Trojan, T. Palasyuk, M. Eremets, R. Cava, S. Naghavi, F. Casper, V. Ksenofontov, G. Wortmann, and C. Felser, arXiv:0903.2143 (unpublished).
[107] S. Masaki, H. Kotegawa, Y. Hara, H. Tou, K. Murata, Y. Mizuguchi, and Y. Takano, arXiv:0903.2594, J. Phys. Soc. Jpn. (to be published).
[108] S. Margadonna, Y. Takabayashi, M. T. McDonald, K. Kasperkiewicz, Y. Mizuguchi, Y. Takano, A. N. Fitch, E. Suard, and K. Prassides, Chem. Commun. (Cambridge) **2008**, 5607.
[109] Y. Mizuguchi, F. Tomioka, S. Tsuda, T. Yamaguchi, and Y. Takano, arXiv:0810.5191 (unpublished).